



# High-content CRISPR screening

Christoph Bock<sup>1,2</sup>✉, Paul Datlinger<sup>1</sup>, Florence Chardon<sup>3</sup>, Matthew A. Coelho<sup>4</sup>, Matthew B. Dong<sup>5,6,7</sup>, Keith A. Lawson<sup>8,9</sup>, Tian Lu<sup>10,11,12</sup>, Laetitia Maroc<sup>13</sup>, Thomas M. Norman<sup>14,15,16</sup>, Bicna Song<sup>17,18</sup>, Geoff Stanley<sup>19</sup>, Sidi Chen<sup>5,6,7</sup>, Mathew Garnett<sup>4</sup>, Wei Li<sup>17,18</sup>, Jason Moffat<sup>8,9,20</sup>, Lei S. Qi<sup>19,21,22</sup>, Rebecca S. Shapiro<sup>13</sup>, Jay Shendure<sup>3,23,24</sup>, Jonathan S. Weissman<sup>14,15,25</sup> and Xiaowei Zhuang<sup>10,11,12</sup>

**Abstract** | CRISPR screens are a powerful source of biological discovery, enabling the unbiased interrogation of gene function in a wide range of applications and species. In pooled CRISPR screens, various genetically encoded perturbations are introduced into pools of cells. The targeted cells proliferate under a biological challenge such as cell competition, drug treatment or viral infection. Subsequently, the perturbation-induced effects are evaluated by sequencing-based counting of the guide RNAs that specify each perturbation. The typical results of such screens are ranked lists of genes that confer sensitivity or resistance to the biological challenge of interest. Contributing to the broad utility of CRISPR screens, adaptations of the core CRISPR technology make it possible to activate, silence or otherwise manipulate the target genes. Moreover, high-content read-outs such as single-cell RNA sequencing and spatial imaging help characterize screened cells with unprecedented detail. Dedicated software tools facilitate bioinformatic analysis and enhance reproducibility. CRISPR screening has unravelled various molecular mechanisms in basic biology, medical genetics, cancer research, immunology, infectious diseases, microbiology and other fields. This Primer describes the basic and advanced concepts of CRISPR screening and its application as a flexible and reliable method for biological discovery, biomedical research and drug development — with a special emphasis on high-content methods that make it possible to obtain detailed biological insights directly as part of the screen.

## Forward genetics

Screening approach in which genes involved in the phenotype of interest are identified by screening genetically perturbed cells.

## Pooled CRISPR screen

A technique in which genetically encoded perturbations are introduced in bulk and read out with sequencing or imaging technology.

## Arrayed CRISPR screens

A technique in which perturbations are introduced in individual reaction compartments and remain physically separated.

✉e-mail: [cbock@cemm.oeaw.ac.at](mailto:cbock@cemm.oeaw.ac.at)

<https://doi.org/10.1038/s43586-021-00093-4>

There is a need in molecular biology and biomedical research for open-ended, hypothesis-generating research, in order to discover previously unknown molecular mechanisms. Genetic screening provides a powerful approach for identifying genes, pathways and mechanisms involved in a given phenotype or biological process. This is illustrated by the many successes of forward genetics in cell lines<sup>1</sup> and in model organisms such as flies<sup>2,3</sup>, worms<sup>4</sup>, yeast<sup>5</sup>, plants<sup>6</sup> and fish<sup>7</sup>, and pioneering work in RNA interference (RNAi) screens<sup>8,9</sup>.

CRISPR screens exploit the efficiency and flexibility of CRISPR–Cas genome editing<sup>10</sup>. They have become a popular and productive tool for biological discovery in a broad range of applications<sup>11,12</sup>. In a typical pooled CRISPR screen (FIG. 1), a CRISPR guide RNA (gRNA) library is introduced in bulk into cells, such that individual cells receive different gRNAs and are perturbed according to the gRNA received by the cell. These gRNAs are usually delivered by lentiviral transduction and are integrated into the DNA of the target cells, making it possible to efficiently determine the induced perturbations based on the gRNA sequence.

The CRISPR–Cas protein is either stably expressed in the cells or ectopically introduced as a plasmid, virus, mRNA or protein. The gene-edited cells are challenged with a selective pressure such as drug treatment, viral infection or cell proliferation, such that the cells compete with each other based on the fitness effect of the engineered genetic perturbations. The gRNAs are then counted in the pool of cells retained after the challenge. This is usually done by high-throughput sequencing. Finally, their representation is compared between different challenges or different time points. In the resulting data, depletion of specific gRNAs identifies genes whose disruption sensitizes cells to the challenge, whereas their enrichment identifies genes whose disruption confers a selective advantage.

In contrast to pooled screens, arrayed CRISPR screens maintain physical separation between perturbations throughout the screen (FIG. 1). As each target gene occupies a separate compartment — for example, different wells on a 96-well plate — arrayed screens tend to be more labour-intensive, costly and limited in scale than pooled screens. Their advantage is that the perturbation

## Author addresses

- <sup>1</sup>CeMM Research Center for Molecular Medicine of the Austrian Academy of Sciences, Vienna, Austria.
- <sup>2</sup>Institute of Artificial Intelligence, Center for Medical Statistics, Informatics, and Intelligent Systems, Medical University of Vienna, Vienna, Austria.
- <sup>3</sup>Department of Genome Sciences, University of Washington, Seattle, WA, USA.
- <sup>4</sup>Wellcome Sanger Institute, Wellcome Genome Campus, Hinxton, UK.
- <sup>5</sup>Department of Genetics, Yale University School of Medicine, New Haven, CT, USA.
- <sup>6</sup>Systems Biology Institute, Yale University, West Haven, CT, USA.
- <sup>7</sup>Center for Cancer Systems Biology, Yale University, West Haven, CT, USA.
- <sup>8</sup>Donnelly Centre, University of Toronto, Toronto, Ontario, Canada.
- <sup>9</sup>Department of Molecular Genetics, University of Toronto, Toronto, Ontario, Canada.
- <sup>10</sup>Howard Hughes Medical Institute, Harvard University, Cambridge, MA, USA.
- <sup>11</sup>Department of Chemistry and Chemical Biology, Harvard University, Cambridge, MA, USA.
- <sup>12</sup>Department of Physics, Harvard University, Cambridge, MA, USA.
- <sup>13</sup>Department of Molecular and Cellular Biology, University of Guelph, Guelph, Ontario, Canada.
- <sup>14</sup>Department of Cellular and Molecular Pharmacology, University of California, San Francisco, CA, USA.
- <sup>15</sup>Howard Hughes Medical Institute, University of California, San Francisco, CA, USA.
- <sup>16</sup>Program for Computational and Systems Biology, Sloan Kettering Institute, Memorial Sloan Kettering Cancer Center, New York, NY, USA.
- <sup>17</sup>Center for Genetic Medicine Research, Children's National Hospital, Washington, DC, USA.
- <sup>18</sup>Department of Genomics and Precision Medicine, George Washington University, Washington, DC, USA.
- <sup>19</sup>Department of Bioengineering, Stanford University, Stanford, CA, USA.
- <sup>20</sup>Institute for Biomaterials and Biomedical Engineering, University of Toronto, Toronto, Ontario, Canada.
- <sup>21</sup>Department of Chemical and Systems Biology, Stanford University, Stanford, CA, USA.
- <sup>22</sup>ChEM-H, Stanford University, Stanford, CA, USA.
- <sup>23</sup>Brotman Baty Institute for Precision Medicine, Seattle, WA, USA.
- <sup>24</sup>Howard Hughes Medical Institute, University of Washington, Seattle, WA, USA.
- <sup>25</sup>Whitehead Institute for Biomedical Research, Cambridge, MA, USA.

a cell receives is predefined by the study design and does not need to be measured explicitly. Therefore, arrayed screens are easier to combine with read-outs that do not involve any sequencing, such as imaging, proteomics and metabolomics profiling.

For reasons of scale and scope, pooled screens are primarily used for discovery, whereas arrayed screens are primarily used for validation and follow-up investigation. Nevertheless, recent technological advances make it possible to obtain detailed biological insights as part of discovery-oriented pooled CRISPR screens. The use of sophisticated models such as organoids and whole organisms, flexible perturbations such as gene activation and repression, diverse biological challenges and data-rich read-outs such as single-cell sequencing and imaging are establishing pooled CRISPR screens as a powerful method for functional biology. Such high-content CRISPR screens provide exciting opportunities to perform mechanistic research at scale.

This Primer introduces concepts, practical considerations and applications of CRISPR screens, with a focus on pooled screens and high-content approaches. We describe how a typical CRISPR screen is designed and executed, including the choice and optimization of the model system. We discuss various CRISPR perturbations such as gene knockout, activation and inhibition, and complex read-outs such as single-cell sequencing and imaging. We outline good practices for analysing

and interpreting data from CRISPR screens, and review groundbreaking applications of CRISPR screening across a broad range of fields. We also describe how CRISPR screens should be documented to enhance their reproducibility and provide lasting value. Finally, we outline current challenges and future developments in the area of high-content CRISPR screening.

## Experimentation

The experimental design of a typical CRISPR screen comprises four main elements (FIG. 1): the biological model; a method for CRISPR-based perturbation; biological challenges that influence the competition among the perturbed cells; and a read-out that connects the observed biological phenotypes to the gRNAs that induced them. The research question typically defines the selection of the right model and the most relevant biological challenges, and recent advances in CRISPR technology and high-throughput profiling provide flexibility for selecting suitable perturbations and read-outs. This section provides an overview of typical CRISPR screens. In addition, a checklist of considerations when starting a CRISPR screen is shown in BOX 1.

## Conducting a pooled CRISPR screen

**Selection of the biological model.** The first step for a successful CRISPR screen is to select a model system that captures the relevant biological processes and is amenable to genetic screening. Immortalized cell lines provide an inexpensive and easy to handle model for studying biological mechanisms that are adequately represented by simple in vitro cultures. To study more complex and context-dependent biological phenomena, screens can be conducted in primary cells, in tissue explants or in stem-cell-derived cultures including organoids. CRISPR screening is also possible in living animals<sup>13</sup>, albeit at a smaller scale than is feasible for in vitro screens. For example, screens in mouse models can be performed by editing cells ex vivo and then transplanting them into the organism, or by delivering the gRNAs and the CRISPR–Cas protein into the mice for in vivo editing.

To enhance the efficiency of CRISPR screening, the target cells can be engineered to express the CRISPR–Cas protein. This way, only the gRNAs need to be delivered ectopically during the screen. This separation can also improve safety as no single construct contains both components needed for inducing double-strand breaks. Clones with high and stable Cas9 expression can be preselected<sup>14</sup>. However, working with just one or a few clones increases the risk of clone-specific artefacts and requires careful validation to ensure that the selected clones are representative and informative for the biological question. For in vivo screens in mice and ex vivo screens in mouse primary cells, transgenic mice can be used that constitutively express Cas9 (REFS<sup>15,16</sup>) or one of its derivatives<sup>17</sup>. For human primary cells, viral delivery of the gRNAs can be combined with transfection of a Cas-encoding plasmid, a chemically modified mRNA or the CRISPR–Cas protein itself<sup>18</sup>.

Careful selection and optimization of the screening model are essential to ensure that the results are broadly

## High-content CRISPR screens

Screens combining complex models, perturbations and stimuli with data-rich read-outs.

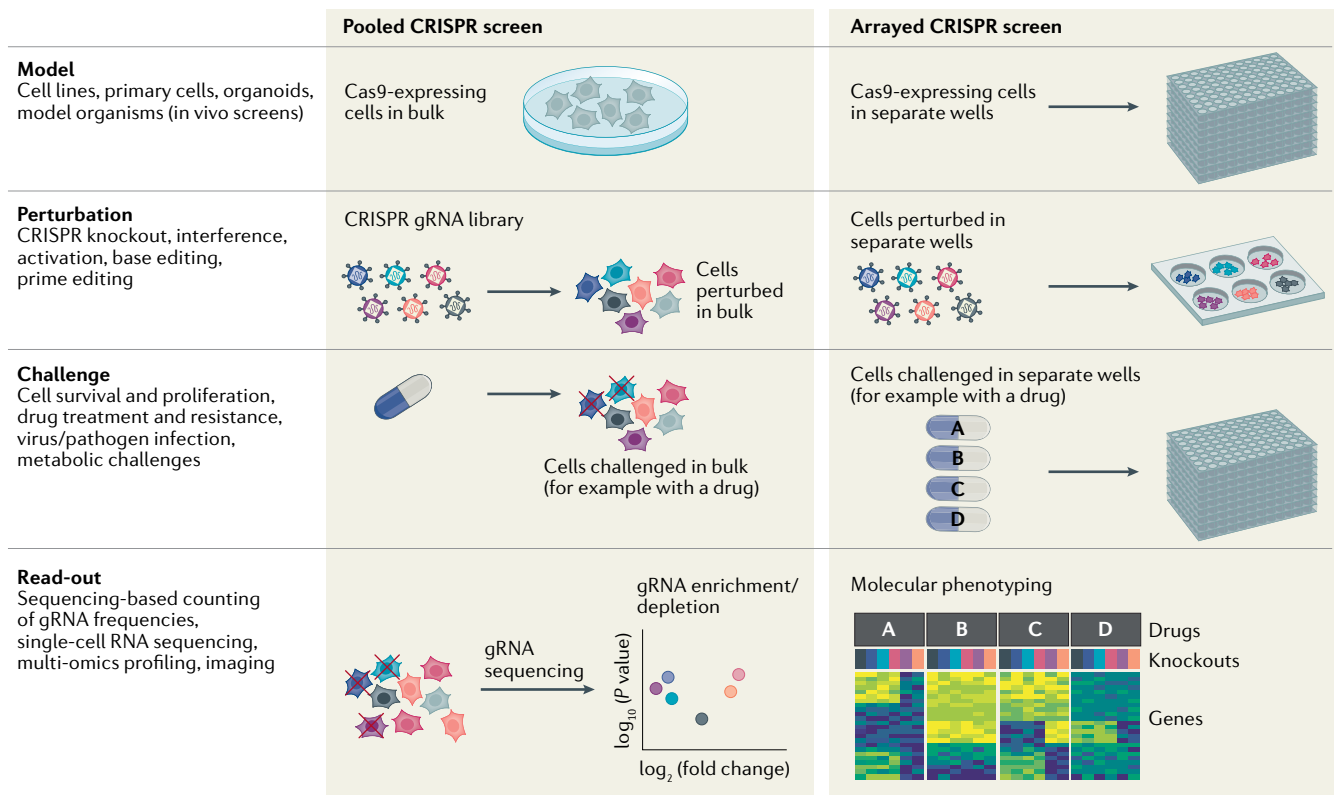


**Fig. 1 | Experimental design for CRISPR screening.** CRISPR screens can be described along four dimensions: the biological model in which the screen is conducted; perturbations introduced using CRISPR technology; challenges to which the perturbed cells are exposed; and a read-out that measures the induced molecular or cellular effects. In pooled CRISPR screens, perturbations are introduced in bulk. They are genetically encoded and typically read out by guide RNA (gRNA) sequencing. In arrayed CRISPR screens, different perturbations are introduced separately — for example, in different wells of a 96-well plate. As each reaction compartment is subjected to a defined perturbation, the read-out does not need to include gRNA sequencing.

relevant to the investigated biological phenomena. It is often advisable to use several variants of the same model — for example, cell lines with different genetic backgrounds — to enhance the relevance and interpretability<sup>19,20</sup>. Such biological replicates are particularly important because the same perturbation may cause different phenotypic consequences depending on the genetic background<sup>21</sup>. CRISPR screens should be performed using at least three biological replicates to obtain robust and interpretable results, although well-designed and carefully implemented screens can produce reliable data with fewer replicates<sup>22</sup>.

**Perturbation and CRISPR library design.** The CRISPR–Cas protein is expressed in the model cells to enable CRISPR-based perturbations. This is done either transiently by introducing the plasmid, mRNA or protein into the cells, or stably by lentiviral transduction or genome engineering, with or without selection or subcloning of individual clones with high CRISPR–Cas protein levels. The efficiency of CRISPR perturbation should be tested and, if necessary, optimized; this can be achieved by delivering gRNAs targeting several test loci by lentiviral transduction<sup>23–25</sup> and evaluating editing efficiency at the DNA level, for example using targeted DNA sequencing. It is also advisable to confirm successful

perturbation at the protein level<sup>26</sup> using techniques such as western blotting or flow cytometry.

For the CRISPR screen, a gRNA library is prepared (FIG. 2) and transduced into the cells in bulk. Most screens target protein-coding genes, although CRISPR screens can also be performed for non-coding DNA and gene regulatory regions<sup>27,28</sup>. CRISPR gRNA libraries may be genome-wide or focused on a smaller set of tens to thousands of genes. Genome-wide screens do not depend on prior knowledge and may reuse existing genome-wide gRNA libraries; however, they require a large number of cells for adequate coverage, which makes them labour-intensive and costly — or even infeasible for rare cell types. Focused screens often provide a useful alternative to genome-wide screens, with the limitation that their scope is restricted to the chosen target genes and that unexpected biological mechanisms are easily missed. It is possible to combine both strategies, by performing a genome-wide screen with modest coverage (which includes all genes but has comparatively low sensitivity for each individual gene) and a targeted screen with high coverage (which focuses on specific candidate genes or gene sets, and thereby achieves higher sensitivity of detection for these genes).

Various tools and resources facilitate the selection of gRNAs for the widely used *Streptococcus*

**Biological replicates**  
Separately conducted repetitions of the same CRISPR screen using cells from different individuals or different passages of a cell line

**Coverage**  
The average number of cells per guide RNA (gRNA) in a CRISPR screen.

**Multiplicity of infection (MOI).** The average number of virions (and, by extension, guide RNAs (gRNAs)) delivered per cell during infection.

#### Genetic interactions

The combined effect of the simultaneous perturbation of several genes, which may deviate from the sum of the individual effects.

#### Positive selection screens

Also known as enrichment screens. Cells with the phenotype of interest are selected (enriched) in the screens; other cells are depleted.

#### Negative selection screens

Also known as dropout screens. Cells with the phenotype of interest are depleted in the screen; other cells are maintained.

*pyogenes*-derived Cas9 protein<sup>22,29–32</sup> and alternatives such as AsCas12a and LbCas12a (REFS<sup>33,34</sup>). For both genome-scale and focused CRISPR knockout (CRISPRko) screens, it is advisable to include at least four different gRNAs for each target gene<sup>32</sup>, although carefully designed and validated gRNA libraries with fewer gRNAs per gene can provide reliable results<sup>35</sup>. All gRNA libraries should include gRNAs for application-specific positive and negative control genes, which are important to validate the screen. In addition, they should include control gRNAs that target known safe harbour loci or other genomic regions where no specific effects of gene editing are expected, in order to account for the DNA damage response and for non-specific reduction in cell proliferation caused by CRISPRko; this is particularly relevant in aneuploid cancer cells<sup>36</sup> or when targeting multiple loci per cell<sup>33,37</sup>.

In pooled CRISPR screens, the gRNA library is typically cloned into a lentiviral vector, and the cells are transfected at a relatively low multiplicity of infection (MOI), often between 0.3 and 0.5. This is to ensure that few cells receive more than one gRNA simultaneously. As a result, it is not usually necessary to account for potential genetic interactions between different gRNAs in

the same cell. Screens with much higher MOIs are being used when cell numbers are limited<sup>38</sup>, when most gRNAs are not expected to have any effect<sup>39</sup> or when studying genetic interactions<sup>40</sup>. As an alternative to combinatorial screens with high MOIs, multiplexed gRNA expression systems provide finer control of gRNA expression. Such screens can be implemented with paired expression cassettes<sup>41–45</sup> or by exploiting the ability of Cas12a to process multiple gRNAs<sup>33,37,46,47</sup>.

The goals of the screen influence the advisable coverage of cells per target gene. For positive selection screens, for example to identify perturbations that confer drug resistance, a coverage of 100–200× per target gene is desired; this can be broken down to 4 gRNAs per gene with 25–50× coverage each. By contrast, negative selection screens tend to require a coverage of 500–1,000× per target gene to detect essential genes with high sensitivity. Bioinformatic tools such as CRISPulator<sup>48</sup> can be used to simulate the effect of different design decisions on the coverage and statistical power of CRISPR screens.

The number of target genes multiplied by the desired coverage provides a rough estimate for the number of cells that must be infected and maintained during the screen. If this estimate exceeds what is practically feasible, it is typically better to select fewer target genes than to run the screen with low coverage and risk poor reproducibility. Once the scale of the screen has been established, it is advisable to perform a series of pilot experiments for optimization, with the goal to achieve high consistency between biological replicates and to minimize unwanted selective pressures, cell stress or population bottlenecks. Moreover, it is important to ensure that cell culture vessels and media changes support the planned cell numbers and growth rates, particularly for large and logistically challenging screens with cell numbers in the hundreds of millions.

**Selection and calibration of the challenge.** In pooled CRISPR screens, the perturbed cells compete with each other for representation in the final pool of cells. By adding a biological challenge that modulates the selective pressures, such screens can be tailored to many different research questions. For biological processes that are closely linked to cell survival and proliferation, unconstrained in vitro proliferation may be sufficient as a challenge, whereas other research questions often require tailored biological challenges such as drug treatment, viral infection or functional assays.

For a successful screen, it is important to understand the dose–response relationship of the challenge, and to calibrate the selective pressures such that the perturbed cells compete with each other in a meaningful way. For negative selection screens, the selection should be mild — for example, using an effective dose of a drug or virus that kills 25–50% of perturbed cells; by contrast, stronger selection with effective doses that kill above 50% of cells is advisable for positive selection screens<sup>49,50</sup>.

The timing of the challenge is an important consideration that can influence the results of CRISPR screens. In screens for essential genes, for example, read-outs at early time points tend to enrich for genes

### Box 1 | Checklist for getting started with CRISPR screening

1. What are the most suitable models and the most relevant phenotypic read-outs for the investigated biological process? Simple read-outs such as cell proliferation or a selectable marker tend to be easier, cheaper and more scalable. By contrast, complex read-outs including single-cell RNA sequencing (RNA-seq) and spatial imaging can provide much more detailed information already as part of the screen.
2. What are realistic cell numbers and what are the proliferation characteristics of the chosen model? What is the largest cell population that can be maintained at acceptable cost and effort throughout the screen?
3. Is the model amenable to lentiviral transduction? If not, which alternative delivery methods might be applicable? For example, what about transient transfection of plasmids, ribonucleoprotein (RNP) complexes or mRNA, or transposon-mediated integration of the Cas protein into the genome? What are suitable delivery vectors? The list of popular plasmids on the website of the non-profit [Addgene](#) repository provides an up-to-date starting point.
4. Has the delivery and perturbation been optimized for best efficiency? Has the model been tested with suitable positive and negative controls and optimized to provide a high signal-to-noise ratio?
5. Considering points 1–4, is the model compatible with genome-wide screening? If not, what is the maximum library size that can be screened with adequate coverage? As a guideline, we recommend a coverage of 100–200 cells per target gene for positive selection screens and 500–1,000 cells per target gene for negative selection screens.
6. What type of guide RNA (gRNA) library is most suitable? Does the selected library include all relevant controls or do they need to be added separately? Genome-wide libraries are readily available from [Addgene](#) and other sources. Nevertheless, many applications benefit from the creation of custom libraries.
7. Before performing the first screen, which gRNAs and genes are expected to be enriched or depleted based on the study design (positive and negative controls) and relevant biological knowledge? After the first screen, did the expected results materialize with good signal-to-noise ratio? If not, what are potential problems and how can the screen be improved?
8. After running the screen in three biological replicates, how consistent are the results? Does the screen need to be optimized and repeated? Which hits are selected for validation? What is the most suitable approach to validating the screening hits — for example, using secondary screens (potentially with high-content read-outs) or using small-scale validation experiments?

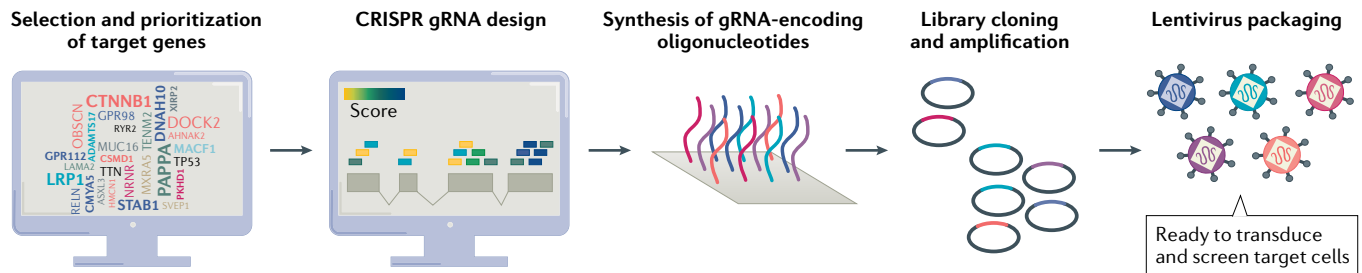


Fig. 2 | **Preparation of CRISPR gRNA libraries.** The guide RNA (gRNA) library defines which genes are probed in a CRISPR screen. Application-specific libraries are designed using bioinformatic tools (detailed in TABLE 1), synthesized as oligonucleotide pools, cloned in bulk into the plasmid vector and packaged into a lentivirus for delivery into cells.

whose knockout causes immediate cell death — such as genes involved in transcription and translation — whereas later time points also identify genes that affect cell proliferation and fitness more indirectly<sup>51</sup>. Inducible Cas9 makes it possible to screen for the early effects of targeting essential genes in genome-wide screens<sup>52</sup> and optogenetic modulation of Cas9 activity enables precise spatio-temporal control of genome editing<sup>53,54</sup>.

**Guide RNA frequency as the screening read-out.** To assess the effect of different perturbations, gRNA frequencies can be counted and compared between conditions. This either includes the entire cell population (as a read-out of cell survival and proliferation) or is artificially restricted to certain cell populations to investigate specific biological phenomena. For example, cells can be enriched based on surface markers or cellular phenotypes prior to gRNA counting. Importantly, the gRNAs in a CRISPR screen both induce the perturbation and serve as genetic barcodes that denote the perturbations that the cells have been exposed to. It is thus possible to obtain a precise quantitative representation of gRNAs by sequencing gRNA amplicon libraries prepared from each analysed sample. The enrichment or depletion of each gRNA and target gene is determined relative to the representation of gRNAs in the gRNA library and by comparing between experimental conditions.

gRNAs targeting control genes with known phenotypic effects are useful for validating the screen, quantifying the signal-to-noise ratio<sup>55–57</sup> and calibrating the selective pressure. It is advisable to perform small test screens that target a handful of positive and negative control genes for different strengths of the challenge and to select the conditions that provide maximum separation of gRNA counts between the positive and negative controls. It can also be useful to perform variations of the same screen with different conditions — for example, different concentrations of a drug — in order to capture the full spectrum of genes that contribute to the biological process of interest<sup>58</sup>. Whereas many CRISPR screens analyse only a single ‘end point’ that has been optimized for best separation between positive and negative controls<sup>59,60</sup>, it can be informative to assess multiple time points to capture dynamic changes over the course of the screen.

When interpreting the results of a pooled CRISPR screen, the target genes are often ranked in order to identify the most promising screening hits for follow-up.

However, even the top-ranking hits may contain false positives, which can arise from biases in the assay or random fluctuations. Moreover, the precise ranking of hits can be noisy even in successful screens. This is particularly true when the observed differences are small. It is advisable to select multiple hits for experimental validation, for example by more focused pooled or arrayed validation screens or small-scale assays, ideally using complementary models and read-outs. Although it is common practice to cherry-pick interesting screening hits for validation, this approach cannot validate the screen as a whole. For a representative assessment of the screening hits, some hits should be selected for validation solely based on their ranks — for example, the top 20 hits as well as 10 hits each around the 5th, 10th, 25th, 50th and 75th percentiles.

### Alternative perturbations

**CRISPR interference and CRISPR activation.** Most CRISPR screens to date have used CRISPRko, where DNA double-strand breaks are induced in a gRNA-directed way and target genes are knocked out, typically as the result of frameshift mutations introduced by the cell’s DNA repair machinery. Beyond CRISPRko, which is based on Cas nucleases, the CRISPR–Cas system can also be used for RNA-directed recruitment of other molecular functions to specific loci in the genome. To that end, a nuclease-deactivated Cas protein that cannot cut DNA — for example, Cas9 endonuclease dead, usually abbreviated as dCas9 — is combined with protein domains that implement the desired function (FIG. 3).

Recruitment of transcriptional repressors enables CRISPR-mediated downregulation of target genes, a technique known as CRISPR interference (CRISPRi); and transcriptional activators enable CRISPR-mediated upregulation, known as CRISPR activation (CRISPRa)<sup>60–67</sup>. In CRISPRi, dCas9 is fused with a Krüppel associated box (KRAB) domain, which represses gene expression when targeted to promoter regions<sup>63,68–71</sup>. As CRISPRi does not induce DNA damage, it is less toxic to cells than CRISPRko<sup>55,72</sup>. Gene repression may yield different phenotypes to gene knockout as it is less prone to activating compensatory pathways<sup>73</sup>. A limitation of CRISPRi compared with CRISPRko is the need for continuous expression of the dCas9 protein and gRNA to maintain inactivation, although recent work shows that long-term stable repression can be achieved by extensive epigenetic

#### Effective dose

The intensity of a perturbation (such as a drug or virus) that causes an effect (such as cell death) in a specified percentage of cells.

#### Screening hits

Target genes identified as being associated with the phenotype of interest in a CRISPR screen.

remodelling at the target sites<sup>74</sup>. In CRISPRa, fusions of dCas9 and the transcriptional activator VP64 have a modest effect on gene activation<sup>63,75</sup>. Improvements include the dCas9–SunTag system, which increases gene activation by recruiting many copies of VP64 (REF.<sup>66</sup>), and the dCas9–VPR system, which combines three activator domains (VP64 and activator domains from the transcription factors p65 and Rta) into a single fusion

protein<sup>60</sup>. Finally, the widely used synergistic activation mediator (SAM) system recruits the two transcription factors HSF1 and p65 to enhance gene activation on top of a dCas9–VP64 fusion<sup>61</sup>.

Cas proteins other than Cas9 have also been adapted for CRISPRi and CRISPRa. Cas12a (previously known as Cpf1) can cleave a single transcript into multiple gRNAs<sup>76</sup>, which facilitates the simultaneous targeting of

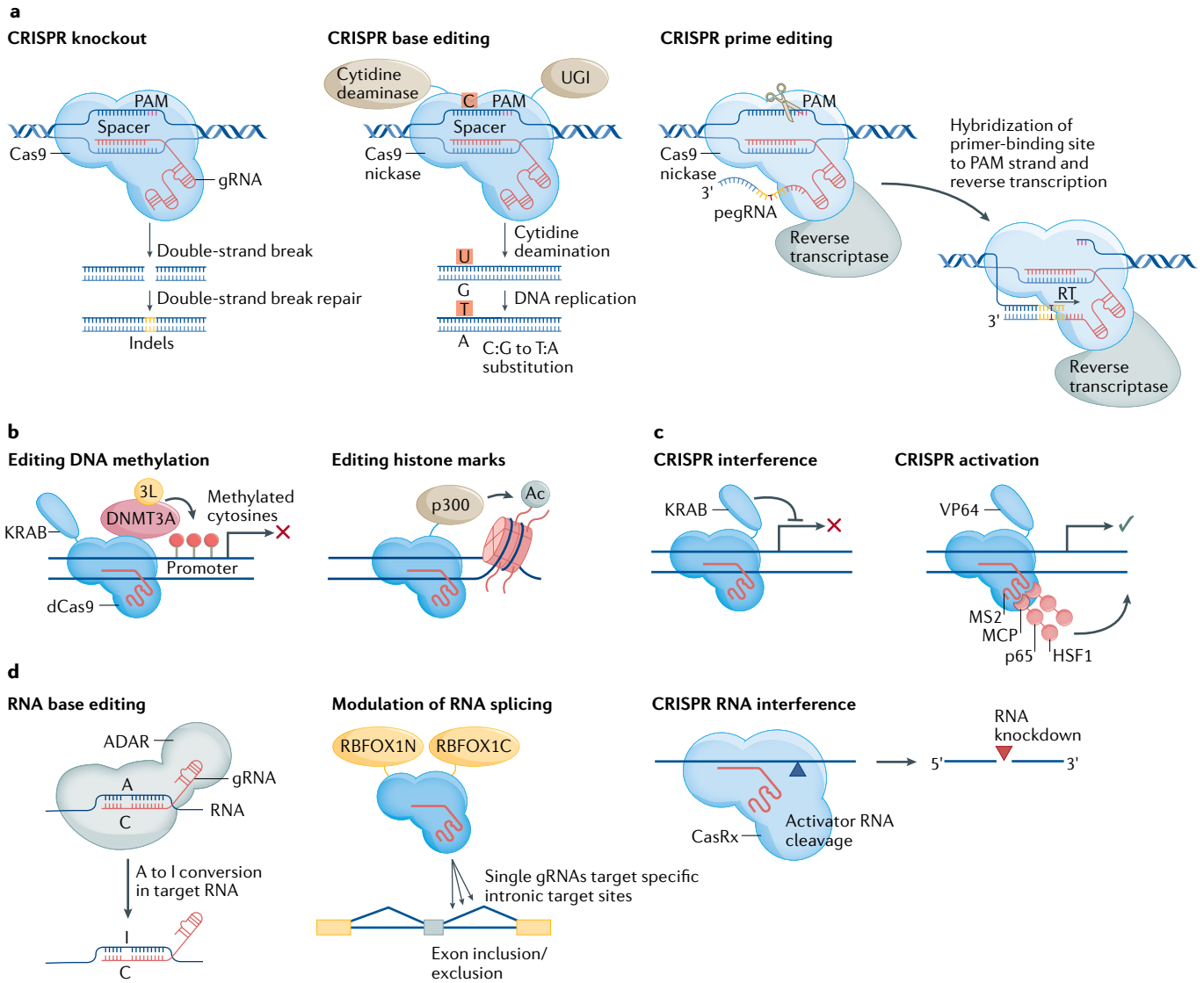


**Fig. 3 | CRISPR-mediated perturbation of cells.** CRISPR technology provides many options to perturb cells. **a** | Genome editing. Directed by a guide RNA (gRNA), Cas9 nucleases introduce double-strand breaks into the target site; subsequent DNA repair results in compromised gene function (CRISPR knockout (CRISPRko)). CRISPR base editors induce specific mutations, by combining a base modification enzyme, a uracil DNA glycosylase inhibitor (UGI) domain that inhibits base excision repair and a Cas nickase that nicks the non-edited strand of DNA to favour repair with the edited base. A cytosine base editor is shown; adenosine base editors are also available. CRISPR prime editing can introduce new sequence information into the genome; it uses a Cas9 nickase fused to a reverse transcriptase and a prime editing gRNA (pegRNA) corresponding to the target locus, which also provides new genetic information. **b** | Epigenome editing. Cas9 endonuclease dead (dCas9) can be combined with epigenetic writer and eraser enzymes such as the demethylase Tet1 (not pictured), the

methyltransferase DNMT3A or the H3K27 acetyltransferase p300 to induce changes in DNA methylation or histone marks. **c** | Transcriptional control. CRISPR interference (CRISPRi) uses dCas9 fused to transcriptional repressors such as Krüppel associated box (KRAB), causing repression of genes close to the gRNA target site. CRISPR activation (CRISPRa) uses dCas9 with transcriptional activators such as the VP64 domain and MCP–p65–HSF1 fusion proteins recruited via an MS2 stem–loop sequence. **d** | RNA modulation. RNA base editors induce specific mutations into RNA molecules using an adenosine deaminase (ADAR) targeted to RNA; it converts adenosine into inosine, which acts as guanine during translation. RNA splicing can be altered at the RNA level by substituting the RNA-binding domain of the RBFOX1 protein with dCas9. Finally, RNA interference (RNAi) can be achieved by a ribonuclease (CasRx) that binds to RNA and cleaves it. PAM, protospacer adjacent motif; RT, reverse transcription.

several genes<sup>77</sup>. dCas12a–VPR and dCas12f–VPR work well as a transcriptional activator, whereas dCas12a–KRAB shows modest repression activity compared with dCas9–KRAB (REFS<sup>77,78</sup>). Further, Cas proteins that target RNA have been fused to transcriptional repressor domains, giving rise to post-transcriptional repression with better specificity than conventional RNAi<sup>79,80</sup>. It is even possible to regulate RNA splicing using CRISPR technology, for example by fusing dCas13d to splicing factors<sup>81</sup> or by editing of splice donor and acceptor sites<sup>82,83</sup>.

CRISPRi and CRISPRa induce epigenetic changes as a side effect of transcriptional repression or activation. In addition, CRISPR technology can be used to directly perturb the epigenome. For example, fusions of dCas9 to epigenetic effectors enable the editing of methylated histone H3K4, H3K9, H3K27, H3K79 and H4K20, acetylated H3K27 and DNA methylation<sup>84–93</sup>. The effects of these epigenetic modifications vary widely in the size of the affected target region (footprint), the stability of the induced changes over time and the strength of the effect, which includes the ability to affect the expression of neighbouring genes. CRISPR has also been used to manipulate the three-dimensional structure of the chromatin, namely by inducing chromatin looping between two genomic loci<sup>94,95</sup> and by recruiting gRNA-specified genomic loci to nuclear structures such as Cajal bodies or the nuclear periphery<sup>96</sup>. Epigenome editing is also feasible for RNA and the epitranscriptome; for example, N<sup>6</sup>-methyladenosine (m<sup>6</sup>A) modifications can be induced by fusing dCas9 with an RNA methyltransferase complex comprising the methyltransferases METTL3 and METTL4 and the splicing regulator WTAP<sup>97,98</sup>.

**Base editing.** CRISPR base editors are fusions of dCas9 with protein domains that chemically modify bases in the DNA; this enables the introduction of genetic changes without inducing double-strand breaks. Base editing has been used to modify disease-associated genetic variants, where it provides better control of the induced changes compared with CRISPRko<sup>99</sup>. Base editing can also be used to perform single-nucleotide-level mapping of regulatory elements, with higher resolution but usually smaller effects than screens using CRISPRi or CRISPRa<sup>100</sup>.

CRISPR base editors typically combine a base modification enzyme that targets single-stranded DNA, a uracil DNA glycosylase inhibitor (UGI) domain that inhibits base excision repair and a Cas9 nickase that nicks the non-edited strand of DNA to trigger repair according to the edited base<sup>99</sup>. Several types of base editors have been developed, changing A to G (adenosine base editors) or C to T (cytosine base editors)<sup>101,102</sup>. Most cytosine base editors use APOBEC1 or CDA1 as the base modification enzyme, and most adenosine base editors use an evolved version of the *Escherichia coli* adenosine deaminase TadA. The efficiency of cytosine base editing was reported to be ~50%, with low indel generation (<1%) and little off-target editing (<1%)<sup>99,103</sup>. Base editing efficiency is lower in post-mitotic cells (~10%), but still more efficient than homology-directed repair in such cells<sup>104</sup>. Although less established than the

systems described above, C to G base editors are also available and can provide high editing efficiency in some instances<sup>105</sup>.

Genome sequence context affects base editing efficiency and needs to be considered during gRNA design<sup>101,102,106</sup>. Most base editors can modify their target base within a small window around the gRNA-encoded genomic position, potentially giving rise to bystander edits<sup>99,103,107</sup>. They can also introduce off-target effects elsewhere in the genome and transcriptome<sup>108</sup>. Base editing of RNA has been demonstrated using a fusion of dCas13b to the adenosine deaminase ADAR2, which converts adenosine into inosine (translationally equivalent to guanine) with an on-target efficiency of ~45% and a low rate of off-target editing<sup>109</sup>. This system was subsequently extended to add cytosine deaminase properties<sup>110</sup>. Owing to constant RNA turnover, RNA editing does not cause permanent changes; therefore, the Cas protein must be expressed throughout the duration of the experiment to maintain the editing effect.

**Insertions and deletions.** CRISPRko introduces small insertions and deletions that typically comprise only a few base pairs. For well-designed gRNAs this is usually sufficient to knock out the target gene, either by introducing frameshift mutations or by disrupting essential protein domains<sup>111</sup>. By contrast, large-scale genome engineering such as insertion or deletion of entire genes requires other methods. One strategy is to induce double-strand breaks at both ends of the target locus, such that the intervening region is either deleted or replaced by a co-delivered homology-directed repair template that carries the desired DNA sequence<sup>112</sup>. However, this method suffers from low efficiency and the need to deliver several matched components to the same cell.

CRISPR prime editing is a promising approach for introducing new DNA sequences into the genome<sup>113</sup>. This method uses a fusion protein comprising dCas9, an engineered reverse transcriptase and a prime editing gRNA (pegRNA) that both encodes the target site and acts as a template for the new genetic information to be introduced into the DNA<sup>113</sup>. Although the initial efficiency of CRISPR prime editing was low, a CRISPRi screen conducted on DNA repair proteins identified DNA mismatch repair as an impediment to prime editing and devised ways to overcome this by transient inhibition of this process or by modification of the pegRNA sequence<sup>114</sup>. The efficiency of prime editing is further enhanced by engineering the pegRNA for higher stability<sup>115</sup>, and there is an increasing collection of software tools that facilitate the design of efficient pegRNAs<sup>116–118</sup>.

A promising application of prime editing is the introduction of many genetic variants in a pooled screen, as represented in a recent preprint article<sup>119</sup>. Although prime editing is generally restricted to short edits of fewer than 20 bp, it is possible to introduce larger genomic deletions by targeting complementary prime editing events on both sides of the target DNA<sup>120,121</sup>. With a similar approach, it is possible to introduce gene-sized DNA fragments into specific loci, for example placing genes in safe harbour loci or tagging proteins with

fluorescent labels<sup>122,123</sup>. These demonstrations of versatility, together with recent gains in efficiency, suggest that CRISPR prime editing screens are becoming broadly useful for investigating complex genetic changes.

### High-content read-outs

**Cell sorting and enrichment.** Counting gRNAs provides a simple and scalable read-out for studying molecular mechanisms linked to cell survival and proliferation. This technique can be generalized to other biological phenomena by sorting or enriching cells with certain biological characteristics (FIG. 4). For example, a reporter cell line can be constructed for a signalling pathway of interest, expressing a fluorescent protein under the control of a promoter that is stably activated by this pathway<sup>124</sup>. Reporter cell lines require extensive validation before use in CRISPR screening to ensure that the activity of the reporter correlates with the biological phenotype of interest and that it provides a sufficient signal-to-noise ratio. Some biological signals are weak and difficult to detect, which has led to the development of synthetic biological circuits for signal amplification<sup>125</sup>.

The enrichment of marker-positive cells is typically performed by fluorescence-activated cell sorting (FACS). One common strategy is to sort cells with high marker expression versus low marker expression (for example, in the top and bottom 1% or 10%, respectively) and to compare gRNA frequencies between these populations. However, processing large numbers of cells using FACS can be time-consuming and costly, especially in the context of genome-wide screens with hundreds of millions of cells. This limitation can be addressed by alternative methods of marker-based cell enrichment based on magnetic beads or microfluidics<sup>126–128</sup>.

Fluorescent dyes can be used to mark specific parts of the cell or to record cell division<sup>129</sup> and fluorescently labelled antibodies can detect proteins of interest, without the need for engineering transgenic reporter cells. This approach has been used in screens of T cell tumour engagement<sup>130</sup>, cancer signalling pathways<sup>131</sup>, immune cell activation<sup>132</sup> and cell differentiation<sup>133–135</sup>. Fluorescence in situ hybridization (FISH) enables quantification of mRNA abundance and can be combined with flow cytometry, which was used in screens for

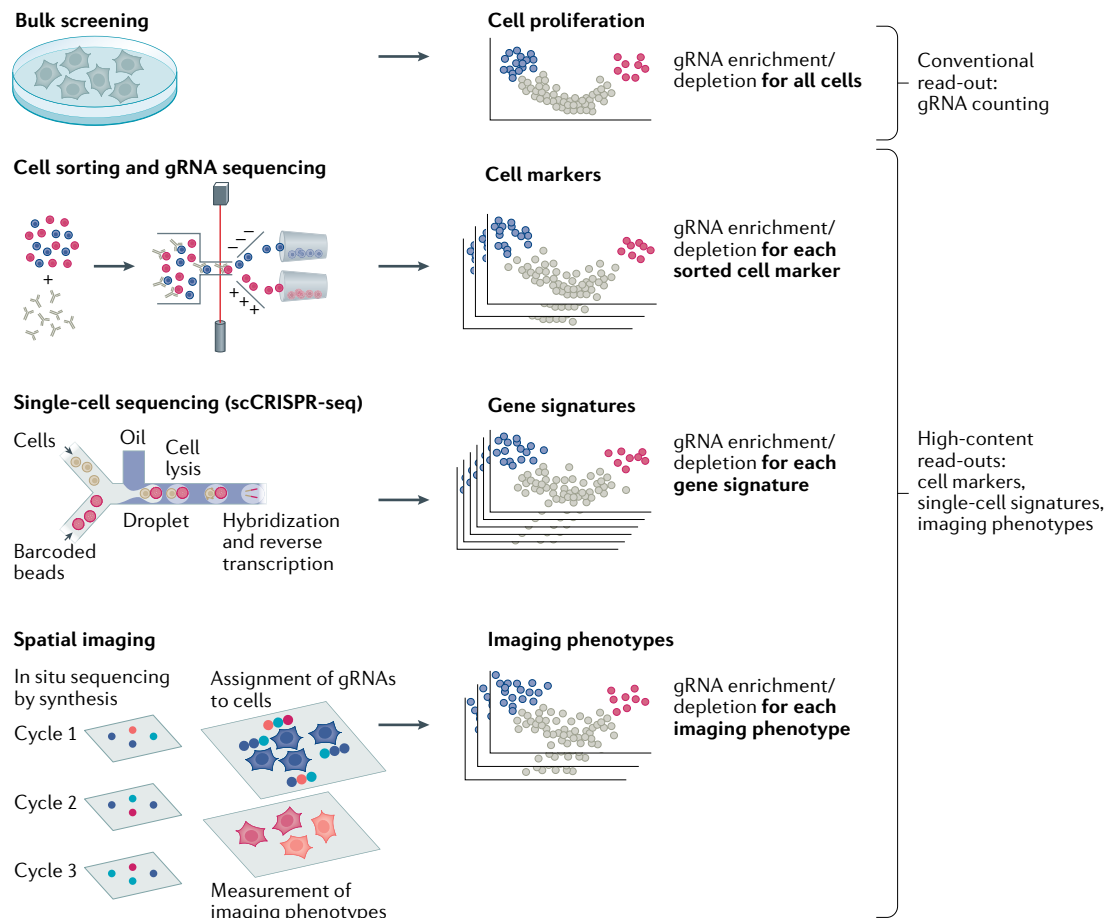


**Fig. 4 | CRISPR screening with high-content read-out.** Sequencing-based counting of guide RNAs (gRNAs) is a straightforward and widely used read-out of pooled CRISPR screens, especially for phenotypes that affect cell proliferation and survival. To broaden CRISPR screening to additional cellular phenotypes, several high-content read-outs have been introduced. Cell sorting prior to gRNA sequencing makes it possible to identify gRNAs and genes that affect predefined, sortable cellular phenotypes — such as expression of a fluorescent reporter. Single-cell sequencing of transcriptomes and matched gRNAs can identify regulators of gene expression and transcriptome-linked cell states. Spatial imaging combined with methods to distinguish gRNAs in individual cells makes it possible to identify genes that affect imaging-based cellular phenotypes, for example inducing changes in cell shape.



**scCRISPR-seq**

An umbrella term for a group of methods that combine pooled CRISPR sequencing with a single-cell sequencing read-out.

regulators of gene expression<sup>136,137</sup>. Further, mass cytometry can facilitate the parallel analysis of many antibodies, enabled by combinatorial labelling of gRNAs with heavy metals to detect them using mass spectrometry<sup>138</sup>.

**Single-cell CRISPR sequencing.** Single-cell sequencing provides a data-rich read-out for CRISPR screens, which is particularly useful for biological phenotypes that are not easily measured by a single marker gene (FIG. 4). CRISPR screens with a single-cell sequencing read-out simultaneously determine the gRNAs that induce a perturbation as well as the corresponding transcriptome profiles in single cells. We refer to this approach as scCRISPR-seq, including methods such as Perturb-seq<sup>139,140</sup>, CRISP-seq<sup>141</sup>, CROP-seq<sup>142</sup> and Mosaic-seq<sup>143</sup>. Transcriptomes provide a particularly high-content read-out for a CRISPR screen, for example allowing scCRISPR-seq screens to determine the type and state of the perturbed cells and to quantify induced changes in gene expression, gene regulatory networks, signalling pathway activity and other properties that can be inferred from the single-cell transcriptomes.

Such scCRISPR-seq screens provide high flexibility for subsequent data analysis; for example, many different virtual screens can be performed on the same scCRISPR-seq data set by assessing gRNA enrichment for different gene signatures, and the data can be re-analysed in light of new biological insights by adding new gene signatures to the bioinformatic analysis, without the need for new experiments. Because scCRISPR-seq screens readily detect differences in cell type among the assayed cells, they are well suited for screens in complex, heterogeneous biological systems such as organoids and primary tissues. The feasibility of *in vivo* scCRISPR-seq has been demonstrated by two studies focusing on the mouse haematopoietic system and the brain<sup>141,144</sup>.

A technical challenge with scCRISPR-seq screens is that CRISPR gRNAs are typically expressed by RNA polymerase III, and therefore not polyadenylated and not captured by standard single-cell RNA sequencing (RNA-seq) assays. This issue can be addressed in several ways. First, individual gRNAs can be linked to matched barcodes that are expressed under an RNA polymerase II promoter and are readily detected by single-cell RNA-seq<sup>139–141,143</sup>. A limitation of this approach is lentiviral ‘template switching’ when preparing gRNA libraries in bulk, which can break the association between gRNAs and expressed barcodes<sup>145</sup>; this can be reduced by decoy transfer plasmids (as shown in a preprint article)<sup>146</sup> or — for small screens — eliminated by preparing the lentivirus in an arrayed format. Second, the CROP-seq vector creates a polyadenylated copy of the gRNA, making it directly readable in single-cell RNA-seq profiles<sup>142</sup>. Third, gRNA capture enables the amplification and sequencing of the gRNAs without the need for a polyadenylation tail<sup>147,148</sup>.

Although genome-wide screens with a single-cell RNA-seq read-out are conceptually feasible, such screens are currently limited by the high cost of single-cell sequencing. Therefore, scCRISPR-seq screens are typically conducted at a scale of up to a few thousand target

genes, for example to validate and better characterize gene sets obtained from genome-wide CRISPR screens, population genomics studies and general biological knowledge.

To reduce sequencing costs, gene panels can be used to assay only genes of specific biological interest<sup>148,149</sup>. Further, scCRISPR-seq screens can be performed with high MOIs, such that most cells carry several perturbations; this is particularly useful when most gRNAs are not expected to have any effect<sup>39</sup>. Finally, cost-effective methods for single-cell RNA-seq such as combinatorial indexing<sup>150,151</sup> and the related scifi-RNA-seq assay<sup>152</sup> will facilitate scCRISPR-seq and arrayed CRISPR screens with millions of single-cell transcriptomes.

The ongoing development of single-cell multi-omics assays<sup>153,154</sup> will likely lead to screens with single-cell read-outs of the genome, epigenome, transcriptome, proteome and/or metabolome. Indeed, scCRISPR-seq screens have already been conducted with a single-cell ATAC-seq read-out, providing insights into the complexities of chromatin regulation<sup>155–157</sup>. Screens with combined measurement of the transcriptome and cell surface protein have also been established<sup>147</sup> and applied to study the regulation of immune checkpoints and genes mediating immune evasion in cancer treatment<sup>158,159</sup>.

**CRISPR screening with spatial imaging read-outs.**

Imaging provides an attractive read-out for CRISPR screens that complements the molecular perspective of single-cell sequencing with a focus on cell morphology (FIG. 4). Exploiting recent advances in imaging technology, it is now possible to assay the localization, transportation and dynamics of individual molecules, molecular assemblies and organelles inside cells, on top of the characterization of cell shape and behaviour.

CRISPR screens with imaging read-outs can be performed in an arrayed format following established concepts from high-content drug screening<sup>160</sup>. In addition, imaging-based pooled CRISPR screens have been demonstrated using several approaches. Following a similar concept to FACS-based screens, cells with specific phenotypes can be identified by imaging, isolated and subjected to gRNA sequencing to determine the genetic perturbations. In one method, this was achieved by culturing cells on arrays containing 40,000 individual microwells, physically isolating microwells that contain cells with the imaging-based phenotype and harvesting them for gRNA sequencing<sup>161</sup>. Using this method, 1,078 RNA-binding proteins were screened for potential roles in stress granule formation. In an alternative method, a photoactivatable protein was selectively illuminated in cells with an imaging-based phenotype of interest, and these fluorescently marked cells were enriched by FACS and subjected to gRNA sequencing<sup>162–164</sup>. This method was used to investigate the subcellular localization of the transcription factor EB<sup>163</sup> and the regulation of nuclear size<sup>164</sup>.

A limitation of imaging followed by cell selection and gRNA sequencing is the small number of cellular phenotypes that can be studied in a single experiment. This limitation is addressed by methods that determine the gRNA identity for each cell directly based on the

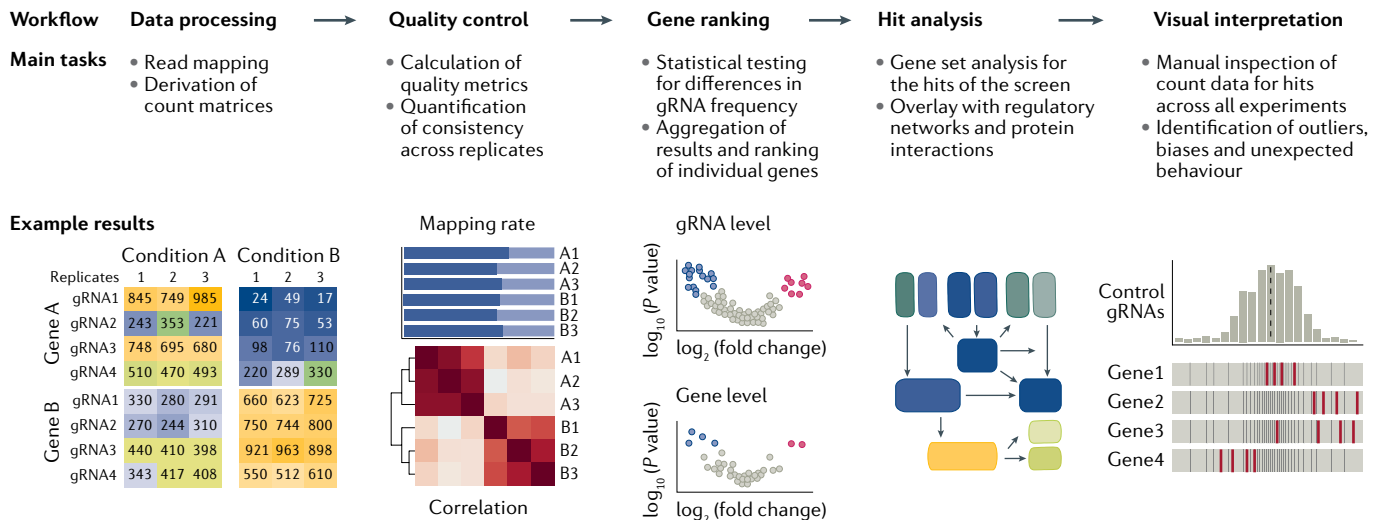


Fig. 5 | **Bioinformatic analysis of CRISPR screening data.** Starting from sequencing data, typical steps in the analysis of a pooled CRISPR screen comprise data processing, quality control, gene ranking, hit analysis and visual interpretation. This workflow is depicted with a description of tasks and an illustration of typical results. gRNA, guide RNA.

imaging data<sup>165,166</sup>. One such method uses a microfluidic chip to randomly seed transfected cells into individual trap chambers, where the cells divide and fill each chamber with clones that share the same perturbation and barcode. The induced phenotypes are observed by imaging, and the barcodes are determined by sequential rounds of FISH imaging<sup>166</sup>. This method was applied to a CRISPRi screen in *E. coli*, investigating the effect of 235 genes on cell division and the location of the replication fork as measured by live-cell imaging<sup>167</sup>. A conceptually similar method uses multiplexed error-robust FISH (MERFISH)<sup>168</sup> to read the barcodes associated with the perturbations<sup>165,169</sup>. This method has been applied to screen 54 RNA-binding proteins for their effect on the localization of long non-coding RNAs in mammalian cells<sup>169</sup>.

Perturbation-specific barcodes can also be determined by in situ sequencing<sup>170</sup>. The barcodes are reverse transcribed, subjected to rolling circle amplification and profiled using in situ sequencing by synthesis<sup>171,172</sup>. This approach was used to analyse 952 genes for potential roles in the nuclear translocation of NF- $\kappa$ B and p65 (REF.<sup>170</sup>). The same study also demonstrated direct in situ sequencing of gRNAs using the CROP-seq vector, which removes the need for perturbation-specific barcodes and may help increase scalability.

## Results

The primary results of CRISPR screens are gRNA counts based on amplicon sequencing for pooled screens with cell survival, proliferation and FACS-based read-outs; single-cell sequencing data for scCRISPR-seq screens; and microscopy data for imaging-based screens. Bioinformatic methods have been developed for analysing and interpreting these results; this typically involves the five main steps of data processing, quality control, gene ranking, hit analysis and visual interpretation (FIG. 5). Multiple open-source software tools are available to support the analysis of CRISPR screens; these are listed in TABLE 1.

## Data processing

Raw data such as sequencing reads or imaging data are processed and converted to count matrices, which form the basis of subsequent analyses. For pooled CRISPR screens with gRNA amplicon sequencing as the read-out, the raw sequencing reads are mapped to a reference of gRNA sequences, either as part of an integrated analysis pipeline such as MAGeCK<sup>173</sup>, CERES<sup>174</sup> or CB2 (REF.<sup>175</sup>), or using standard sequence alignment tools such as Bowtie<sup>176</sup> or BWA<sup>177</sup>. The result is a matrix that contains count data for each analysed gRNA. For scCRISPR-seq screens, the gRNA sequences and single-cell sequencing data are typically processed separately and connected using unique cell barcodes. Processing of the single-cell sequencing data follows established practices<sup>178,179</sup> with bioinformatic software tools such as Seurat<sup>180</sup>, ScanPy<sup>181</sup> and Monocle<sup>150</sup>. Imaging-based screens can build on the extensive methodology for analysing high-throughput imaging data<sup>182</sup>, including software tools such as CellProfiler<sup>183</sup> and EBImage<sup>184</sup>. However, these tools do not explicitly account for gRNA detection and analysis, and custom processing scripts are required to annotate the single-cell sequencing or imaging data with the corresponding gRNAs as the basis for further analysis.

## Quality control

Quality control is essential for reliable downstream analysis. Relevant quality metrics for pooled CRISPR screens include the average read and/or cell coverage per gRNA, the percentage of missing gRNAs and the evenness of read coverage across gRNAs as measured by the Gini coefficient<sup>185</sup>. The consistency of the results across biological replicates can be evaluated by analysing pairwise correlations and visualizing the global similarity of all experiments, for example using principal component analysis. It is advisable to compare the depletion of known essential genes against non-essential genes to determine the effectiveness of the perturbations<sup>57,186</sup>.

Table 1 | Software tools for analysing CRISPR screens

Method	Language	Raw data processing	Quality control	Guide RNA efficiencies	Negative controls	Correction for copy number	Visualization	Application/description
<i>Tools for analysing pooled CRISPR screens</i>								
BAGEL2 (REF. <sup>328</sup> )	Python	–	Yes	–	–	Yes (with CRISPRcleanR)	–	Identification of fitness genes and tumour suppressors in genome-wide CRISPRko screens
CRISPRBetaBinomial <sup>175</sup>	R	Yes	Yes	–	Yes	–	Yes (with CRISPRCloud)	Quantification of gRNA abundances based on the $\beta$ -binomial distribution
CRISPhieRmix <sup>187</sup>	R, C++	–	–	Yes	Yes	–	Yes	Modelling guide efficiency in CRISPRi/CRISPRa screens using hierarchical mixture models
CRISPR-SURF <sup>329</sup>	Python	Yes	–	–	–	–	Yes	Discovery of gene regulatory elements based on CRISPR tiling screens
CRISPRcleanR <sup>191</sup>	Python, R	Yes	Yes	–	–	Yes	Yes	Identification of essential genes with unsupervised correction of biases owing to copy number
crispy <sup>190</sup>	Python	–	Yes	–	–	Yes	–	Correction for gene-independent fitness effects owing to copy number/structural rearrangements
gscreend <sup>189</sup>	R	–	Yes	–	–	–	Yes	Statistical modelling of population bottlenecks on gRNA frequency in CRISPR screens
JACKS <sup>193</sup>	Python	–	–	Yes	Yes	–	–	Bayesian method for joint analysis of different screens using the same gRNA library
MAGeCK <sup>173</sup>	Python	Yes	–	Yes	Yes	Yes	–	Model-based approach to identify essential genes and pathways
MAGeCK-VISPR <sup>185</sup>	Python	Yes	Yes	Yes	Yes	Yes	Yes	Workflow for quality control, analysis and visualization of CRISPR screening data
MAGeCKFlute <sup>194</sup>	R	–	Yes	Yes	Yes	Yes	Yes	Integrated software pipeline for CRISPR screens that includes MAGeCK and MAGeCK-VISPR
<i>Tools for (meta-)analysis of large-scale CRISPR screening data sets</i>								
CERES <sup>174</sup>	R	Yes	Yes	Yes	–	Yes	–	Estimation of gene dependency from essentiality screens while correcting for copy number
Chronos <sup>330</sup>	Python	–	–	–	–	Yes	–	Modelling cell proliferation to improve the identification of hits from large-scale screening data

Table 1 (cont.) | Software tools for analysing CRISPR screens

Method	Language	Raw data processing	Quality control	Guide RNA efficiencies	Negative controls	Correction for copy number	Visualization	Application/description
<i>Tools for (meta-)analysis of large-scale CRISPR screening data sets (cont.)</i>								
CoRe <sup>331</sup>	R	–	–	–	–	–	Yes	Identification of constitutively essential genes from multiple CRISPR screens
<i>Tools for analysing combinatorial CRISPR screens</i>								
GEMINI <sup>237</sup>	R	–	–	–	–	–	–	Identification of genetic interactions from combinatorial CRISPR screens with a Bayesian approach
Orthrus <sup>332</sup>	R	Yes	Yes	–	Yes	–	Yes	Processing, scoring and analysis of combinatorial CRISPR screening data
<i>Tools for analysing CRISPR screens with a single-cell sequencing read-out (scCRISPR-seq)</i>								
FBA <sup>197</sup>	R	Yes	Yes	–	–	–	–	Processing and analysis of feature barcodes in single-cell RNA-seq data, including CRISPR perturbations
MELD <sup>196</sup>	Python	–	–	–	–	–	Yes	Analysing experimental perturbations in single-cell RNA-seq data using manifold learning
MIMOSCA <sup>140</sup>	Jupyter Notebook	–	–	–	–	–	–	Estimating the effect of CRISPR perturbations in single-cell RNA-seq data using regularized linear models
Mixscape <sup>159</sup>	R	–	–	Yes	Yes	–	Yes	Improving the signal-to-noise ratio in scCRISPR-seq data by removing confounding sources of variation
MUSIC <sup>333</sup>	R	–	–	Yes	Yes	–	Yes	Integrated pipeline for model-based analysis of scCRISPR-seq data
Normalisr <sup>334</sup>	Python	–	–	–	–	–	–	Normalization and statistical association testing for single-cell RNA-seq and scCRISPR-seq data
scMAGeCK <sup>335</sup>	Python, R	Yes	–	Yes	Yes	–	Yes	Identification of genes associated with multiple expression phenotypes in scCRISPR-seq data

CRISPRa, CRISPR activation; CRISPRi, CRISPR interference; CRISPRko, CRISPR knockout; gRNA, guide RNA; RNA-seq, RNA sequencing.

Finally, screens that involve single-cell sequencing or imaging data should undergo corresponding quality control<sup>178,179,182</sup>, including bioinformatic detection of potential technical artefacts and correction for batch effects. **BOX 2** provides a list of important quality control criteria for pooled CRISPR screens.

### Gene ranking

Following quality control, gRNAs and their target genes or genomic regions are ranked according to their effect on the phenotype of interest. For pooled screens with

an amplicon sequencing read-out, these phenotypes are typically defined by the stimuli and conditions in the study design. For scCRISPR-seq and imaging-based screens, they can be derived from the high-content data — for example by unsupervised clustering or supervised classification of cell states based on gene signatures<sup>139–142</sup> or spatial location<sup>141,142,170</sup>. Enrichment/depletion scores and corresponding *P* values are calculated for each phenotype, gRNA and target gene using statistical approaches such as negative binomial, Bayesian or hierarchical mixture models, which may account for

variability in gRNA efficiency<sup>185,187,188</sup>, off-target effects<sup>174</sup> and the effect of population bottlenecks<sup>189</sup>.

To improve gene ranking, many software packages including MAGeCK<sup>173</sup>, CERES<sup>174</sup>, CRISPY<sup>190</sup> and CRISPRcleanR<sup>191</sup> statistically correct for DNA copy number variation, which is a relevant source of bias in CRISPR screens for cell survival and proliferation in cancer cell lines<sup>36</sup>. These tools use existing profiles of copy number variation (where available) or estimate this effect from gRNAs that target nearby genomic locations in genome-scale libraries. Differences in gRNA efficiency can affect the gene ranking, and statistical models have been developed to model such variability and to account for off-target effects<sup>187,192</sup>. For robust and interpretable results it is useful to compare gRNA frequencies across related conditions. Several software packages provide built-in support for different study designs, including paired samples, multiple time points or alternative treatment conditions<sup>185,193,194</sup>. For example, MAGeCKFlute<sup>194</sup> and DrugZ<sup>195</sup> were designed for the common scenario of comparing gRNA frequencies between two conditions (for example, screens of drug-treated and untreated cells). Finally, dedicated software tools have been developed for the analysis of scCRISPR-seq screens, which account for heterogeneity among perturbed cells<sup>140,159,194,196,197</sup>.

### Hit analysis

Once target genes have been ranked by their enrichment/depletion score, the top hits can be assessed in terms of plausibility and biological relevance. Such manual inspection is assisted by online resources including PubMed, Ensembl, GeneCards, ClinVar, OMIM and COSMIC. To detect biological patterns that are shared among several top hits, it can be informative to perform enrichment analyses using databases such as MSigDB<sup>198</sup> and STRING<sup>199</sup>, and software tools such as Enrichr for genes<sup>200</sup> and LOLA for genomic regions<sup>201</sup>. For the most interesting hits of a CRISPR screen, it is advisable to

manually review the abundance of the corresponding gRNAs across all tested conditions. Highly variable gRNA frequencies across biological replicates can be an indicator of a noisy and unreliable screen, and gRNA enrichment or depletion among the negative controls may point to technical biases affecting the results.

### Visual interpretation

Visualizations facilitate the biological interpretation of CRISPR screens. A heat map of sample correlations helps evaluate consistency across biological replicates and the global differences between conditions. Receiver operating characteristic curves are used to assess the sensitivity and specificity of essential gene depletion, a widely useful metric of data quality. Scatter plots of gRNA counts or log fold changes visualize the top hits in the context of the screen's background. Differences between two conditions can also be visualized using volcano plots, which plot gRNA counts or log fold changes against their associated *P* values. Many software tools for CRISPR data analysis include dedicated visualization modules (TABLE 1). For example, the R functions of MAGeCKFlute can help visualize screening results for individual genes across multiple experimental conditions<sup>194</sup>. Using such visualizations for individual target genes is often useful for assessing the enrichment/depletion of all gRNAs targeting those genes. For example, consistent behaviour across different gRNAs targeting the same gene supports the validity of a top hit, whereas outliers and inconsistent results may raise caution about a hit's reliability.

### Applications

The versatility and discovery power of CRISPR screening is demonstrated by its wide range of applications, which include the investigation of fundamental molecular mechanisms, genetic diseases, processes relevant to cancer, immune regulation and microbiology (FIG. 6).

### Molecular and cell biology

Pooled CRISPR screens with simple gRNA count-based read-outs have uncovered genes involved in fundamental biological processes such as transcription regulation<sup>202,203</sup>, epigenetic mechanisms<sup>204</sup>, protein production<sup>205,206</sup>, cell signalling<sup>207,208</sup>, proliferation<sup>209,210</sup> and differentiation<sup>211,212</sup>. Such screens have also identified regulators of cellular organelles such as mitochondria<sup>124,213</sup>, lysosomes<sup>214</sup>, proteasomes<sup>52</sup> and the autophagosome<sup>215,216</sup>. scCRISPR-seq screens have been used to dissect transcription-regulatory processes associated with dendritic cell stimulation<sup>140</sup>, T cell receptor (TCR) induction<sup>142</sup> and epithelial to mesenchymal transition<sup>217</sup>. Further, CRISPR screens with imaging read-outs have investigated regulators of NF- $\kappa$ B translocation<sup>170</sup>. As single-cell sequencing and imaging read-outs do not depend on cell proliferation, they are applicable to perturbations that do not cause cell death and cell types that are naturally post-mitotic; for example, a scCRISPR-seq screen examined how autism-linked genes affect cell types and states in the brain<sup>144</sup>.

Most CRISPR screens target only one gene per cell; this facilitates data analysis but makes it difficult to

#### Box 2 | Quality control criteria for pooled CRISPR screens

- The guide RNAs (gRNAs) should have sufficient representation in sequencing data. It is recommended to have an average of 300–500 sequencing reads per gRNA in each sample.
- Essential genes should be depleted relative to non-essential genes and negative control gRNAs<sup>186</sup>. If no such depletion is seen, the efficiency of the perturbation should be tested in more detail.
- Most non-essential genes and negative control gRNAs should have sufficient sequencing coverage (several hundred reads) and no systematic enrichment or depletion. Strong deviations may indicate that the effective number of cells in the screen is too low, in which case the measured gRNA frequencies may be dominated by random clonal drift.
- Positive and negative control genes selected based on prior biological knowledge should show the expected behaviour, such as gRNA enrichment or depletion in the perturbed cells. If this is not the case, the screen may need further optimization or the chosen model does not recapitulate the investigated biological process well enough.
- Replicates of the screen should show high coherence in terms of the changes in gRNA representation. Low coherence is indicative of a poor signal-to-noise ratio, which can arise not only from high noise levels (for example, owing to random clonal drive as the result of insufficient coverage) but also from low signal (for instance, when the perturbations have little effect on the cells' response to the challenge).

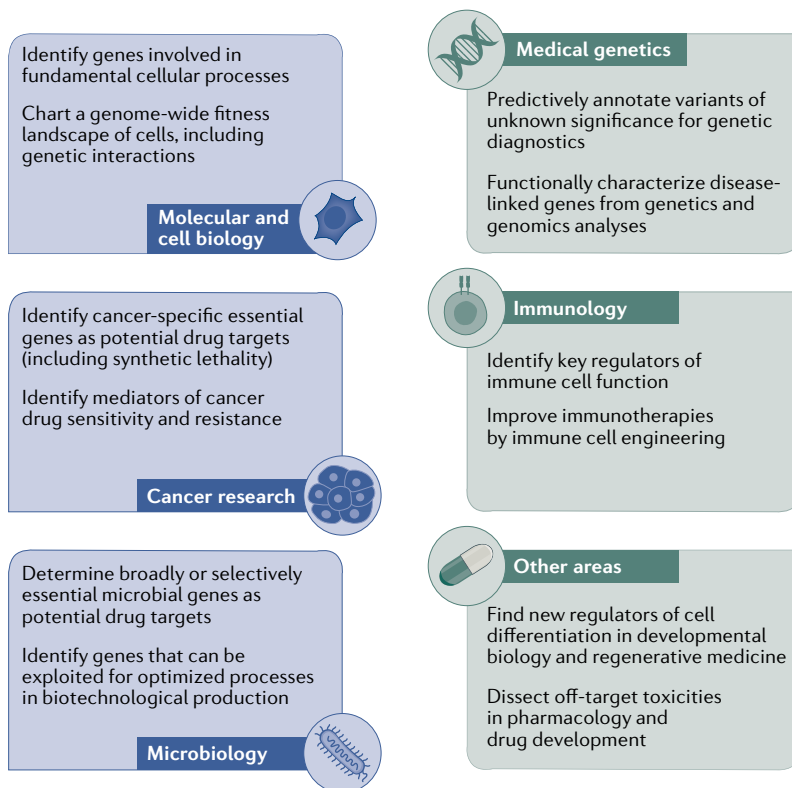


Fig. 6 | **Applications of CRISPR screening.** CRISPR screens are broadly contributing to our understanding of biology. Carefully designed screens can help address a wide range of research topics, some of which are outlined here.

dissect biological processes characterized by redundancy<sup>218–221</sup>, where a phenotypic effect may be detected only when several paralogous genes are perturbed simultaneously. Accounting for redundancy is important for understanding quantitative traits and genetic diseases<sup>222,223</sup> and can be exploited for combination therapies<sup>224</sup>. Pooled CRISPR screens focusing on genetic interactions have mapped more than 200,000 gene pairs in cell lines<sup>44</sup> and several hundred gene pairs in vivo in mice<sup>47</sup>. Single-cell sequencing read-outs have helped dissect complex, non-additive effects on cell state in the context of combinatorial gene regulation<sup>140</sup> and the unfolded protein response<sup>139</sup>. More recently, scCRISPR-seq was used to profile hits from a CRISPRa screen to identify genetic interactions that drive differentiation to specific cell types<sup>225</sup>. For complex molecular and cellular read-outs, two genes may synergize with respect to some aspects of their induced transcriptomes, while acting antagonistically with regards to other aspects. Computational methods for manifold learning may help interpret genetic interaction data based on scCRISPR<sup>225</sup> and imaging read-outs<sup>226</sup>, towards the goal of inferring models of genetic interactions that are both predictive and interpretable<sup>227</sup>.

#### Medical genetics and rare genetic diseases

CRISPR screening facilitates the annotation of disease-linked genes and genetic variants, specifically by assessing the biological function of variants of uncertain significance in disease-causing genes<sup>228</sup>. Deleterious genetic variants

in *BRCA1* are a risk factor of breast cancer with high clinical relevance, yet many variants are too rare to assess based on medical genetics data alone whether the variant is pathogenic or benign. This challenge has been tackled by saturation genome editing, using CRISPR and homology-directed repair to introduce several thousand single-nucleotide variants into the *BRCA1* locus and measuring their effect in vitro<sup>229</sup>. Further, cytosine base editors have been used to assess genetic variants in *BRCA1* and *BRCA2* (REFS<sup>230,231</sup>), and a recent study extended this approach to 86 genes involved in the DNA damage response<sup>232</sup>.

Not all genetic variants can be targeted with base editors owing to their sequence specificity and the need for a Cas-specific PAM sequence close to the target site. Nevertheless, a gRNA library has been developed that targets more than 50,000 ClinVar variants with base editing<sup>230</sup>, and CRISPR prime editing promises to provide even more flexibility to engineer a wide range of genetic variants across the genome<sup>113</sup>.

CRISPR screening is useful for the functional analysis of genetic variants associated with polygenic diseases, including risk alleles identified through genome-wide association studies (GWAS) and population genome sequencing. Such studies have statistically linked thousands of genomic regions to a wide range of diseases and human phenotypes, although their rate of pinpointing causal variants and underlying mechanisms has been low. CRISPR screens can complement genetic association studies by testing the biological function of a large number of genetic variants in parallel before labour-intensive investigation of individual variants. In one such screen, gRNAs were tiled across the *BCL11A* enhancer to map which parts of this enhancer are associated with fetal haemoglobin expression, which may be therapeutically relevant for  $\beta$ -thalassaemia and sickle cell anaemia<sup>233</sup>. Another study applied CRISPRi screens with a FISH read-out of target gene expression to quantify gene regulatory effects for thousands of candidate enhancer–gene pairs<sup>136</sup>.

A challenge of using CRISPR screens for assaying genetic variants is the need to develop and validate specific reporter assays for each gene or phenotype of interest. This can be avoided with scCRISPR-seq, exploiting the versatility of transcriptional profiles as correlates of diverse cellular phenotypes. For example, CRISPRi followed by a single-cell RNA-seq read-out was used to measure the effect of enhancer silencing on the transcriptome<sup>143</sup> and to obtain single-cell profiles for the effect of several thousand enhancers in a single experiment<sup>39</sup>. This approach is capable of linking genetic variants to the genes they regulate, which is an important task given that most disease-linked genetic variants identified by GWAS lie in non-coding genomic regions.

#### Cancer research

CRISPR screens are well suited for studying cancer biology given the wide range of available models and the cancer relevance of readily screenable phenotypes such as cell proliferation and drug resistance. Initial studies focused on mapping essential genes in cancer cell

#### Manifold learning

A set of machine learning methods that seek to uncover hidden structures in the data through dimensionality reduction.

#### Variants of uncertain significance

Genetic variants for which there is insufficient genetic evidence to support or exclude a causal phenotypic effect.

#### Saturation genome editing

Introduction of many genome edits into a gene or regulatory element, with the goal of comprehensively assessing their phenotypic impact.

lines<sup>57,59</sup>, following the hypothesis that cancer-specific gene essentiality may indicate worthwhile drug targets. CRISPR screens have been performed in hundreds of cancer cell lines<sup>21,51,57,174,220</sup>, making it possible to distinguish between cancer-specific effects and core essential genes, and to study the context dependence of gene essentiality. It has been predicted from RNAi data that at least a thousand cancer cell lines need to be screened to observe most cancer-relevant gene dependencies at least once<sup>234</sup> and it will take many more to chart reliable genetic fitness landscapes of cancer cells. Encouragingly, CRISPR screening data have been successfully aggregated across different laboratories<sup>20,235</sup>, suggesting that large-scale efforts that combine data across multiple sites are feasible.

CRISPR screens conducted in isogenic pairs of cancer cell lines<sup>220,236</sup> provide a powerful tool to identify cases of synthetic lethality<sup>237</sup>. As many cancers lack dominant, druggable oncogenes for targeted therapy, one promising approach is to identify genes that are non-essential but synthetic lethal with cancer-specific gene alterations that are not themselves druggable. This concept is illustrated by the synthetic lethal effect of PARP1 inhibition in *BRCA1/BRCA2* mutant cancers<sup>238,239</sup>. CRISPR screens recently identified a potent synthetic lethal interaction between the helicase-encoding *WRN* gene and microsatellite instability<sup>21,240–242</sup>.

CRISPR screens in cancer cell lines are broadly useful for investigating tumour-specific biological processes, including oncogenic transcription regulation<sup>243</sup>, hypoxia<sup>58</sup>, metabolic stress<sup>244</sup>, cytokines<sup>19</sup>, immune evasion<sup>245,246</sup> and DNA damage<sup>247,248</sup>. However, certain aspects such as metastasis and the tumour microenvironment are difficult to model in vitro. To address these limitations, CRISPR screens have been performed using mouse models of cancer<sup>19,133,249</sup>, either based on engraftment of gene-edited cells or in vivo genome editing. Because the number of cells that engraft or are edited in vivo is typically low, such screens tend to be limited to a few hundred target genes. Cancer organoids have the potential to combine certain advantages of in vivo models including their three-dimensional structure with those of in vitro models, such as high throughput and easy access for perturbations. Indeed, organoids have a greater overlap with the in vivo properties of human tumours than cancer cell lines and have helped uncover relevant cancer vulnerabilities<sup>35,250,251</sup>.

CRISPR screens also provide new insights into therapeutically relevant mechanisms. In immuno-oncology, they found that tumour immune evasion occurs through diverse mechanisms including Ras signalling, interferon, antigen presentation, autophagy and epigenetic remodelling<sup>19,50,129,130,249,252</sup>. Relevant to molecularly targeted therapy, a CRISPR screen that challenged cells with the BRAF inhibitor vemurafenib found that depletion of neurofibromin, merlin and the mediator complex component MED12 conferred drug resistance in BRAF-mutant melanoma cells<sup>29,210</sup>. Similarly, mutagenesis of the proteasome component PSMB5 in a base editing screen revealed novel mutations that confer resistance to the cancer drug bortezomib<sup>253</sup>.

## Immunology

CRISPR screens for immunological mechanisms can be conducted in primary immune cells by exploiting methods for efficient delivery of Cas9 and gRNAs<sup>209,254</sup>. For example, the SLICE method combines lentiviral delivery of gRNAs into stimulated human CD8<sup>+</sup> T cells with electroporation of the cells to introduce the Cas9 protein<sup>129,255</sup>. This method led to the identification of genes that modulate the proliferation response of CD8<sup>+</sup> T cells<sup>129</sup>. CRISPR screens in primary T cells have identified new genes involved in T cell proliferation<sup>129</sup>, activation<sup>132</sup> and antitumour activity<sup>130,131,256,257</sup>. Further, screens in dendritic cells stimulated with bacterial lipopolysaccharide (LPS) uncovered novel regulators of Toll-like receptor 4 (TLR4) signalling<sup>258</sup>, and screens in macrophages identified genes involved in inflammasome activation and other inflammatory pathways<sup>259,260</sup>. CRISPR screens have also identified host factors involved in SARS-CoV-2 viral infection, contributing to our understanding of host cell entry and exit, and virus replication<sup>261–269</sup>.

Pooled CRISPR screens are generally restricted to studying cell-intrinsic regulatory mechanisms; by contrast, arrayed CRISPR screens support the investigation of cell-extrinsic effects and complex immune cell interactions<sup>270</sup>. Further, in vitro screens are usually performed in super-physiological conditions and may overestimate perturbation effects. For example, TCR activation assays use a bead-based method for immune stimulation, which does not adequately recapitulate the complexities of the immunological synapse<sup>271</sup>. These challenges can be addressed by in vivo CRISPR screens<sup>130,133,257,272,273</sup>, either in immunocompetent mice for a focus on murine immune cells, or in immunodeficient or humanized mice with xenotransplanted human immune cells<sup>274</sup>. Such screens may provide insights into tissue-resident immune cells<sup>275</sup> and the role of structural cells such as epithelial cells, endothelial cells and fibroblasts<sup>276</sup>, which have not yet been a focus of in vivo CRISPR screening.

There are multiple challenges faced by in vivo screens. First, delivery of the CRISPR machinery can be challenging and inefficient in living animals; hence, it is often advisable to use transgenic mice that constitutively express the Cas protein. Second, in vivo screens are more limited in scale compared with in vitro screens; it is therefore important to define relevant target genes. Data from the ImmGen consortium<sup>277</sup>, the Human Cell Atlas<sup>278</sup>, the BLUEPRINT project<sup>279</sup>, public databases and the scientific literature can facilitate the design of application-specific gRNA libraries for in vivo screens in haematopoietic cells. Third, the antigenic repertoire of T cells and B cells can affect clonal dynamics independent of the CRISPR-induced perturbations and add noise to the screen, thus requiring multiple replicates.

## Microbiology

CRISPR screens are broadly useful for microbiological applications, including the analysis of animal and plant pathogens and the development of new biotechnological tools for food production, waste treatment and pharmaceutical manufacturing (FIG. 7). CRISPR technology has enabled the genetic manipulation of microbial species that were considered genetically

### Synthetic lethality

Special case of a genetic interaction in which knockouts of two genes are individually tolerated, but their combination is lethal to cells.

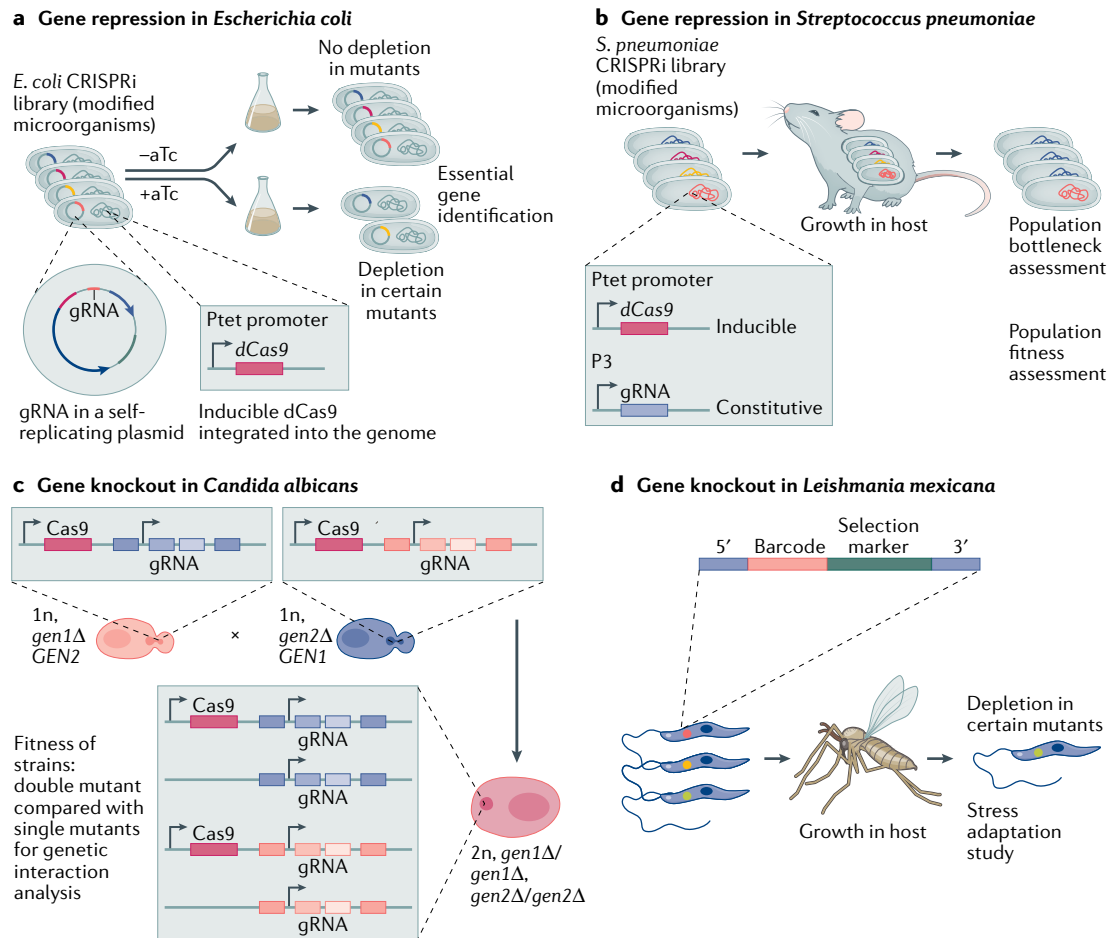


**Fig. 7 | Applications of CRISPR screening in diverse microorganisms. a** | Gene repression by CRISPR interference (CRISPRi) facilitated genome-wide screening for essential genes in the model organism *Escherichia coli*<sup>283</sup>. In the depicted system, the guide RNA (gRNA) sequence is constitutively expressed from a replicating plasmid, while the Cas9 endonuclease dead (dCas9) gene is integrated in the bacterial genome under an inducible Ptet promoter. Gene repression is induced by addition of anhydrotetracycline (aTc), an antibiotic derivative of tetracycline. **b** | A similar inducible CRISPRi approach was used in the bacterial pathogen *Streptococcus pneumoniae* to study population bottlenecks during in vivo infection of a murine host<sup>290</sup>. **c** | CRISPR knockout (CRISPRko) enabled the large-scale construction of double mutants to map genetic interactions in the yeast pathogen *Candida albicans*<sup>280</sup>. **d** | CRISPRko screening and barcode tagging of clones in the parasite *Leishmania mexicana* uncovered genes involved in stress adaptation during sandfly infection<sup>336</sup>.

intractable, including species of bacteria, fungi and parasites<sup>280,281</sup>. CRISPRi-based gene knockdown is predominantly used for screens in microbiology because it circumvents potential species-specific differences in homologous recombination and the repair of double-strand breaks.

Early examples of CRISPR screens in bacteria included CRISPRi-based analysis of non-coding RNAs in *E. coli*<sup>282</sup> and identification of host factors relevant to bacteriophage infection for improving phage therapy<sup>283</sup>. These studies challenged the essentiality of genes previously characterized by transposon insertion sequencing (Tn-seq) and established CRISPRi as a complementary method for identifying essential genes in both model and non-model bacteria. For example, a CRISPRi-based analysis of *Bacillus subtilis*<sup>284</sup> was extended to diverse species of Firmicutes and Gammaproteobacteria<sup>285</sup>, and a comparative CRISPRi analysis of gene essentiality included diverse isolates of *E. coli*<sup>286</sup>. CRISPR screens also identified condition-specific essential

genes in *Mycobacterium smegmatis*<sup>287</sup> and in the marine bacterium *Vibrio natriegens*<sup>288</sup>.

One key advantage of CRISPR-based methods in microbiology is their robustness across a wide range of species<sup>289</sup>. This has enabled the discovery of novel virulence mechanisms for bacterial pathogens such as *Streptococcus pneumoniae*<sup>290</sup> and technically challenging pathogenic fungi<sup>291</sup> and parasites<sup>292</sup>. For example, CRISPR screens identified virulence factors in *Toxoplasma gondii*<sup>293,294</sup>, *Candida albicans*<sup>295,296</sup> and *Cryptococcus neoformans*<sup>297</sup>. CRISPR screening can also help identify novel targets for antimicrobial drugs based on gene essentiality<sup>282–284</sup> in pathogens such as *S. pneumoniae*, *Streptococcus mutans* and *Vibrio cholerae*<sup>298–300</sup>. CRISPR screens have been used to identify complex genetic interactions and synthetic lethality<sup>295,296,301,302</sup>, novel targets for combination antimicrobial therapeutics<sup>303</sup>, genetic determinants of resistance to existing antimicrobial therapeutics<sup>296,302,304</sup> and mechanisms of bacterial resistance to bacteriophage infection<sup>305</sup>. Finally,



**False positives**

Putative CRISPR screening hits that do not validate, which can be caused by technical biases.

**False negatives**

Potential CRISPR screening hits that would have validated but were missed, which can be caused by suboptimal screening conditions.

it is possible to combine pathogen screens with screens of human host factors<sup>306</sup>.

Beyond microbial pathogens, CRISPR screening can help identify key factors in industrially relevant microorganisms with the goal of optimizing bioprocesses<sup>282,307–311</sup>. For example, genome-wide CRISPRi screening in *E. coli* identified new genes that confer resistance to isobutanol and furfural, which are important traits for biofuel production<sup>282</sup>. Pooled CRISPRi-based screens in *Synechocystis* spp. cyanobacteria have been used to increase productivity and tolerance for L-lactate, which is an important compound for renewable plastics<sup>309,310</sup>. In *Saccharomyces cerevisiae*, a gene knockdown library identified genes involved in furfural tolerance<sup>307</sup>.

Advances in CRISPR technology broaden the scope for CRISPR screening in microbiology. A recent study combined CRISPRi and CRISPRa for genome-wide titration of gene expression in *S. cerevisiae*<sup>311</sup>, and a modified CRISPRi platform with mismatched gRNAs enabled fine-grained control of gene expression in *B. subtilis* and *E. coli*<sup>312</sup>. CRISPRi has been combined with the fluorescent TIMER protein and FACS enrichment in *E. coli* to identify slow-growing mutant strains with high metabolic activity<sup>313</sup>. Multilocus CRISPR editing with homologous recombination has been optimized for use in *E. coli*<sup>308</sup> and *S. cerevisiae*<sup>314</sup>, and applied as a molecular barcoding tool to study genotype–phenotype relationships. Finally, CRISPR base editors have been used to assess the effect of genetic variants on the *S. cerevisiae* proteome at single-residue resolution<sup>315</sup>. Finally, it is possible to combine pathogen screens with screens of human host factors<sup>306</sup>.

**Reproducibility and data deposition**

CRISPR screens are sometimes performed with little consideration for assay optimization and reproducibility, essentially relying on follow-up experiments to obtain robust results for a small subset of manually selected hits. Although this approach has been successful in some cases, it does not realize the full potential of CRISPR screens as a method for systematic biological discovery. Poorly conducted screens can have many false positives, which add to the validation burden and potentially yield spurious patterns of biological enrichment among the hits of the screen. Moreover, they tend to produce false negatives, compromising the screen's ability to provide a reliable list of genes that have a strong effect in the investigated model.

To quantify and enhance reproducibility, CRISPR screens should be conducted with at least three biological replicates and the results should be compared using quantitative metrics such as correlation coefficients and receiver operating characteristic curves. Further, the most interesting hits should be validated with complementary assays. This selection should include some randomly selected hits in order to counter expert selection bias. Complementary to the in-depth validation of a few hits, medium-scale validation screens with high-content read-outs such as single-cell RNA-seq or imaging can help investigate a broader range of hits than is feasible with small-scale assays. This

strategy can also provide an estimate for the false positive rate of the primary screen<sup>258</sup>. Whenever possible, validations should include additional gRNAs to assess off-target effects, or use alternative perturbations — for example, CRISPRa or CRISPRi following a primary screen using CRISPRko. On the computational side, reproducibility can be improved by using workflow management systems such as Snakemake<sup>316</sup> for data processing and R/Python notebooks for documentation of the analysis.

An essential aspect of reproducibility is proper documentation of the screening data and the experimental and computational workflows, such that other researchers can verify and build upon the results. Raw and processed data from each published screen — including the raw sequencing reads, count matrices, ranked and annotated lists of hits, and global metrics of screening performance — must be deposited in suitable data repositories together with a detailed description of the experiment. Raw and processed data should be submitted to the [NCBI Gene Expression Omnibus \(GEO\)](#) or the [EBI ArrayExpress](#) database. Alternatively, raw sequencing data can be submitted to the [International Nucleotide Sequence Database Collaboration](#), which comprises the [NCBI Sequence Read Archive \(SRA\)](#), the [EBI European Nucleotide Archive \(ENA\)](#) and others. Submission to the [EBI European Genome-phenome Archive \(EGA\)](#) or the [NCBI database of Genotypes and Phenotypes \(dbGAP\)](#) may be preferred or required for screens performed on primary human cells or human tissue to comply with data protection regulations. Additional raw and processed data that do not fit into any application-specific database can be submitted to all-purpose repositories such as [Zenodo](#).

There is currently a lack of established community standards for the documentation of CRISPR screens. In particular, no reporting standard exists for CRISPR screens that would correspond to standardization efforts in other areas of high-throughput biology, such as the [Minimum Information About a Microarray Experiment \(MIAME\)](#), [Minimum Information About a Next-generation Sequencing Experiment \(MINSEQE\)](#) and [Minimum Information About a Proteomics Experiment \(MIAPE\)](#) guidelines. In the absence of a widely accepted community standard, [BOX 3](#) provides a brief outline of specific points that we consider important for reporting a CRISPR screen, in order to enhance reproducibility.

Carefully conducted and well-documented CRISPR screens can be highly reproducible across replicates and across laboratories. This was confirmed by a comparative analysis of two large CRISPR screening data sets for cancer cell lines generated independently by the Broad Institute and the Sanger Institute, which identified essential genes with high reproducibility<sup>20,235</sup>. Despite many differences between the reagents and methodologies used to generate these data sets, variation between the two data sets were largely attributed to gRNA library design and differences in the duration of the screens following CRISPRko, which are experimental sources of variation that can be mitigated with appropriate study design and validated methodology.

**Box 3 | Suggested minimum reporting standards for pooled CRISPR screens****Information on the cell or animal model**

- Description of the model including relevant literature references
- Details on how to obtain or recreate the model (reproducibility)
- Characterization of the model including genetic background
- Description of the experimental conditions to prepare the model for the screen

**Information about the gRNA library and CRISPR delivery vectors**

- Description of the guide RNA (gRNA) library (including the gRNA sequences and their targets) and CRISPR delivery vectors (including plasmid maps and cloning method)
- Existing resources: precise indication of which resources were used and from where they were obtained
- Custom resources: submission of libraries and plasmids to a public repository such as [Addgene](#)
- Documentation of validations including sequencing data for libraries and plasmids

**Information on the stimulus**

- Description of the stimulus including detailed experimental protocols
- Documentation of validation and calibration experiments for the stimulus

**Information on the read-out**

- Description of the read-out of the screen (including protocols and reagents), the data obtained and the computational analysis
- Raw and processed FACS, sequencing or imaging data provided in a public repository
- Analysis source code provided as a permanent archive (for example, in [Zenodo](#) or as a supplementary file in a publication) or in a version-controlled open code repository such as [GitHub](#) or [BitBucket](#)

The accumulation of raw CRISPR screening data sets in public databases provides interesting opportunities for meta-analysis of genotype–phenotype relations. Dedicated databases have been developed to find, retrieve and analyse these data sets. The [DepMap](#) resource provides CRISPR screening data and associated genomic profiles for hundreds of cancer cell lines; the CRISPR-view database provides a standardized reanalysis of published CRISPR screening data sets using the [MAGeCK-VISPR](#) pipeline<sup>317</sup>; and the [BioGRID ORCS](#) database collects and curates CRISPR screening data sets from the scientific literature<sup>318</sup>.

**Limitations and optimizations**

A successful CRISPR screen depends on the combination of a suitable biological model, efficient perturbation of the target genes, well-calibrated stimuli and a read-out that captures relevant biological processes. Each of these aspects comes with certain limitations, which can be addressed by careful optimization.

Efficient delivery of the Cas protein and the gRNAs can be a challenge and needs careful optimization, especially for CRISPR screens in primary cells and in vivo. Further, some experimental models are characterized by strong population bottlenecks — for example, only a few cells engraft in most xenotransplantation models. In such cases, genetic drift and selective forces unrelated to the CRISPR-induced perturbation may dominate the analysis and cause high levels of noise. It is therefore important to minimize all population bottlenecks that are unrelated to the screened phenotype; this can be achieved by optimizing cell viability in vitro or engraftment rates in vivo, and by selecting a

sufficiently low number of target genes to ensure adequate coverage.

CRISPRko is a mature technology with high efficiency and few off-target effects; however, a subset of the perturbed cells may retain target protein function owing to in-frame editing. Within CRISPR screens, it is usually not possible to verify the edits made in individual cells, although scCRISPR-seq provides some opportunities in this regard. In-frame editing is therefore difficult to exclude and can reduce the screen's signal-to-noise ratio. For alternative perturbations such as CRISPRi and CRISPRa, selecting a suitable gRNA design can be challenging and is often cell type-specific<sup>30,187,319</sup>. Where possible, gRNAs should be validated in the cell type of interest, for example by measuring their effect on the expression of their respective target genes in arrayed experiments<sup>225</sup>. Alternative perturbations also tend to suffer from stronger off-target effects than CRISPRko<sup>320</sup>.

Most stimuli that have been used in CRISPR screens impose strong selective pressures in a setting of rapidly growing cell lines cultured in nutrient-rich media. Although this set-up has identified important biological mechanisms, the physiological challenges faced by cells in vivo are often less pronounced, are longer lasting and occur in an environment with a comparatively low cell growth rate and nutrient supply. It usually takes careful optimization to calibrate the stimuli in a CRISPR screen in a way that maximizes physiological relevance.

A key limitation of gRNA amplicon sequencing as the screening read-out is that it reduces the screen's biological complexity to measuring only one-dimensional RNA enrichment/depletion scores. High-content read-outs with single-cell sequencing or imaging provide much more detail on the perturbed cells but are limited by their complexity and assay costs. Finally, simple sequencing-based read-outs cannot readily detect clonal outgrowth and PCR amplification artefacts, which can be addressed by perturbation and sequencing protocols that incorporate unique molecular identifiers to distinguish individual editing events<sup>38,321,322</sup>.

**Outlook**

Genetic screens play a major role in shaping our understanding of biology. Over the past two decades, RNAi and gene-trap screens have established the feasibility of genome-wide screens in mammalian cells; and CRISPR–Cas has emerged as a highly efficient perturbation tool that can be programmed with gRNA and read out with sequencing. These developments have dramatically increased the power of genetic screens for biological discovery across a broad range of models. We anticipate that progress in models, perturbations, stimuli and read-outs will continue to enhance the practical utility and discovery power of CRISPR screening.

In terms of new models, it is useful to look beyond cancer cell lines, which have been by far the most widely used biological model in the first wave of CRISPR screens. For example, organoids replicate important aspects of human physiology and pathophysiology in vitro and are amenable to CRISPR screening<sup>250,323–325</sup>. Humanized mice enable in vivo screens of human immune cells, helping to dissect species-specific

**Population bottlenecks**  
Reductions in the genetic diversity among a pool of cells owing to external events.

**Genetic drift**  
Genetic changes over time in a pool of cells, caused by random and uncontrolled events.

**Unique molecular identifiers**  
Short barcodes that uniquely identify individual DNA or RNA molecules.

differences in the regulation of the immune system<sup>326,327</sup>. As CRISPR screening technology works well across various species, there are unique opportunities to apply CRISPR screens in emerging model organisms with interesting biological properties or biotechnological applications, ranging from mammals to microorganisms.

New methods for CRISPR-based perturbation complement established CRISPRko technology and provide additional options for the manipulation of cell states. Once current challenges of efficiency and reliable gRNA design are resolved, powerful gain-of-function screens will be possible using CRISPRa and comprehensive characterization of regulatory regions and epigenetic cell states will be achievable using epigenome editing. Further, CRISPR screening with base editors, homologous recombination and prime editing will enable the functional analysis of a wide range of potentially disease-linked genetic alterations at high resolution and throughput.

Much potential lies in broadening the range of cellular stimuli used in CRISPR screens. The first generation of pooled CRISPR screens exposed cell lines to competitive growth conditions or challenged them with drugs or viruses; now, methods and practices have advanced enough to apply CRISPR screens to milder and more complex challenges. For example, cells can be exposed to specific microenvironments, metabolites or cell–cell interactions. Cells can also be challenged in terms of their regulatory plasticity, ability to adapt to dynamically changing environmental conditions and response

to paracrine signalling in heterogeneous biological models, with applications in areas such as immuno-oncology and regenerative medicine.

Although well-designed pooled CRISPR screens with gRNA counting as their read-out continue to be broadly useful, screens with high-content read-outs such as single-cell sequencing and imaging can provide additional insights into molecular mechanisms already as part of the screen. Such screens do not require the ex ante selection of markers; rather, they support rapid computational iteration of hypotheses and analyses based on the screening data. High-content screens have so far focused mainly on preselected sets of candidate target genes; however, cost-effective high-throughput assays make it possible to screen gene sets comprising several thousand genes with adequate coverage — for example, including all kinases, transcription factors or cellular transporters. Given their flexibility, robustness and biological depth, it seems possible that such high-content screens will eventually become the primary method of CRISPR screening.

In summary, we describe the building blocks of effective CRISPR screening across a wide range of applications. High-content CRISPR screens conducted in complex biological models with single-cell sequencing or imaging read-outs provide a versatile approach for functional analysis at scale, bridging the gap between genome-wide descriptive assays and small-scale mechanistic dissection.

Published online: 10 February 2022

- Grimm, S. The art and design of genetic screens: mammalian culture cells. *Nat. Rev. Genet.* **5**, 179–189 (2004).
- St Johnston, D. The art and design of genetic screens: *Drosophila melanogaster*. *Nat. Rev. Genet.* **3**, 176–188 (2002).
- Wieschaus, E. & Nüsslein-Volhard, C. The Heidelberg screen for pattern mutants of *Drosophila*: a personal account. *Annu. Rev. Cell Dev. Biol.* **32**, 1–46 (2016).
- Jorgensen, E. M. & Mango, S. E. The art and design of genetic screens: *Caenorhabditis elegans*. *Nat. Rev. Genet.* **3**, 356–369 (2002).
- Forsburg, S. L. The art and design of genetic screens: yeast. *Nat. Rev. Genet.* **2**, 659–668 (2001).
- Page, D. R. & Grossniklaus, U. The art and design of genetic screens: *Arabidopsis thaliana*. *Nat. Rev. Genet.* **3**, 124–136 (2002).
- Patton, E. E. & Zon, L. I. The art and design of genetic screens: zebrafish. *Nat. Rev. Genet.* **2**, 956–966 (2001).
- Boutros, M. & Ahringer, J. The art and design of genetic screens: RNA interference. *Nat. Rev. Genet.* **9**, 554–566 (2008).
- Mohr, S. E., Smith, J. A., Shamu, C. E., Neumüller, R. A. & Perrimon, N. RNAi screening comes of age: improved techniques and complementary approaches. *Nat. Rev. Mol. Cell Biol.* **15**, 591–600 (2014).
- Jinek, M. et al. A programmable dual-RNA-guided DNA endonuclease in adaptive bacterial immunity. *Science* **337**, 816–821 (2012).
- Doench, J. G. Am I ready for CRISPR? A user's guide to genetic screens. *Nat. Rev. Genet.* **19**, 67–80 (2018).
- Shalem, O., Sanjana, N. E. & Zhang, F. High-throughput functional genomics using CRISPR–Cas9. *Nat. Rev. Genet.* **16**, 299–311 (2015).
- Kuhn, M., Santinha, A. J. & Platt, R. J. Moving from in vitro to in vivo CRISPR screens. *Gene Genome Editing* **2**, 100008 (2021).
- Fernandes Neto, J. M. et al. Optimized Cas9 expression improves performance of large-scale CRISPR screening. Preprint at *bioRxiv* <https://doi.org/10.1101/2021.07.13.452178v1> (2021).
- Chu, V. T. et al. Efficient CRISPR-mediated mutagenesis in primary immune cells using CrispRGold and a C57BL/6 Cas9 transgenic mouse line. *Proc. Natl Acad. Sci. USA* **113**, 12514–12519 (2016).
- Platt, R. J. et al. CRISPR–Cas9 knockin mice for genome editing and cancer modeling. *Cell* **159**, 440–455 (2014).
- Gemberling, M. P. et al. Transgenic mice for in vivo epigenome editing with CRISPR-based systems. *Nat. Methods* **18**, 965–974 (2021).
- van Haasteren, J., Li, J., Scheideleer, O. J., Murthy, N. & Schaffer, D. V. The delivery challenge: fulfilling the promise of therapeutic genome editing. *Nat. Biotechnol.* **38**, 845–855 (2020).
- Lawson, K. A. et al. Functional genomic landscape of cancer-intrinsic evasion of killing by T cells. *Nature* **586**, 120–126 (2020).
- Pacini, C. et al. Integrated cross-study datasets of genetic dependencies in cancer. *Nat. Commun.* **12**, 1661 (2021).
- Behan, F. M. et al. Prioritization of cancer therapeutic targets using CRISPR–Cas9 screens. *Nature* **568**, 511–516 (2019).
- Hart, T. et al. Evaluation and design of genome-wide CRISPR/SpCas9 knockout screens. *G3* **7**, 2719–2727 (2017).
- Moffat, J. et al. A lentiviral RNAi library for human and mouse genes applied to an arrayed viral high-content screen. *Cell* **124**, 1283–1298 (2006).
- Naldini, L. et al. In vivo gene delivery and stable transduction of nondividing cells by a lentiviral vector. *Science* **272**, 263–267 (1996).
- Zufferey, R., Nagy, D., Mandel, R. J., Naldini, L. & Trono, D. Multiply attenuated lentiviral vector achieves efficient gene delivery in vivo. *Nat. Biotechnol.* **15**, 871–875 (1997).
- Smits, A. H. et al. Biological plasticity rescues target activity in CRISPR knock outs. *Nat. Methods* **16**, 1087–1093 (2019).
- Esposito, R. et al. Hacking the cancer genome: profiling therapeutically actionable long non-coding RNAs using CRISPR–Cas9 screening. *Cancer Cell* **35**, 545–557 (2019).
- Shukla, A. & Huangfu, D. Decoding the noncoding genome via large-scale CRISPR screens. *Curr. Opin. Genet. Dev.* **52**, 70–76 (2018).
- Doench, J. G. et al. Optimized sgRNA design to maximize activity and minimize off-target effects of CRISPR–Cas9. *Nat. Biotechnol.* **34**, 184–191 (2016).
- Horlbeck, M. A. et al. Compact and highly active next-generation libraries for CRISPR-mediated gene repression and activation. *eLife* **5**, e19760 (2016).
- Michlits, G. et al. Multilayered VBC score predicts sgRNAs that efficiently generate loss-of-function alleles. *Nat. Methods* **17**, 708–716 (2020).
- Sanson, K. R. et al. Optimized libraries for CRISPR–Cas9 genetic screens with multiple modalities. *Nat. Commun.* **9**, 5416 (2018).
- Gonatosopoulos-Pournatzis, T. et al. Genetic interaction mapping and exon-resolution functional genomics with a hybrid Cas9–Cas12a platform. *Nat. Biotechnol.* **38**, 638–648 (2020).
- Liu, J. et al. Pooled library screening with multiplexed Cpf1 library. *Nat. Commun.* **10**, 3144 (2019).
- Gonçalves, E. et al. Minimal genome-wide human CRISPR–Cas9 library. *Genome Biol.* **22**, 40 (2021).
- Aguirre, A. J. et al. Genomic copy number dictates a gene-independent cell response to CRISPR/Cas9 targeting. *Cancer Discov.* **6**, 914–929 (2016).
- Gier, R. A. et al. High-performance CRISPR–Cas12a genome editing for combinatorial genetic screening. *Nat. Commun.* **11**, 3455 (2020).
- Zhu, S. et al. Guide RNAs with embedded barcodes boost CRISPR-pooled screens. *Genome Biol.* **20**, 20 (2019).
- Gasperini, M. et al. A genome-wide framework for mapping gene regulation via cellular genetic screens. *Cell* **176**, 377–390.e19 (2019).
- Dixit, A., Kuksenko, O., Feldman, D. & Regev, A. Shuffle-Seq: en masse combinatorial encoding for *n*-way genetic interaction screens. Preprint at *bioRxiv* <https://doi.org/10.1101/861443v1> (2019).
- Diehl, V. et al. Minimized combinatorial CRISPR screens identify genetic interactions in autophagy. *Nucleic Acids Res.* **49**, 5684–5704 (2021).
- Du, D. et al. Genetic interaction mapping in mammalian cells using CRISPR interference. *Nat. Methods* **14**, 577–580 (2017).
- Han, K. et al. Synergistic drug combinations for cancer identified in a CRISPR screen for pairwise genetic interactions. *Nat. Biotechnol.* **35**, 463–474 (2017).
- Horlbeck, M. A. et al. Mapping the genetic landscape of human cells. *Cell* **174**, 953–967.e22 (2018).

45. Shen, J. P. et al. Combinatorial CRISPR–Cas9 screens for de novo mapping of genetic interactions. *Nat. Methods* **14**, 573–576 (2017).
46. Campa, C. C., Weisbach, N. R., Santinha, A. J., Incarnato, D. & Platt, R. J. Multiplexed genome engineering by Cas12a and CRISPR arrays encoded on single transcripts. *Nat. Methods* **16**, 887–893 (2019).
47. Chow, R. D. et al. In vivo profiling of metastatic double knockouts through CRISPR–Cpf1 screens. *Nat. Methods* **16**, 405–408 (2019).
48. Nagy, T. & Kampmann, M. CRISPulator: a discrete simulation tool for pooled genetic screens. *BMC Bioinformatics* **18**, 347 (2017).
49. Kearney, C. J. et al. Tumor immune evasion arises through loss of TNF sensitivity. *Sci. Immunol.* **3**, eaar3451 (2018).
50. Patel, S. J. et al. Identification of essential genes for cancer immunotherapy. *Nature* **548**, 537–542 (2017).
51. Tzelepis, K. et al. A CRISPR dropout screen identifies genetic vulnerabilities and therapeutic targets in acute myeloid leukemia. *Cell Rep.* **17**, 1193–1205 (2016).
52. de Almeida, M. et al. AKIRIN2 controls the nuclear import of proteasomes in vertebrates. *Nature* **599**, 491–496 (2021).
53. Bubeck, F. et al. Engineered anti-CRISPR proteins for optogenetic control of CRISPR–Cas9. *Nat. Methods* **15**, 924–927 (2018).
54. Carlson-Stevermer, J. et al. CRISPRoff enables spatio-temporal control of CRISPR editing. *Nat. Commun.* **11**, 5041 (2020).
55. Gilbert, L. A. et al. Genome-scale CRISPR-mediated control of gene repression and activation. *Cell* **159**, 647–661 (2014).
56. Birsoy, K. et al. An essential role of the mitochondrial electron transport chain in cell proliferation is to enable aspartate synthesis. *Cell* **162**, 540–551 (2015).
57. Hart, T. et al. High-resolution CRISPR screens reveal fitness genes and genotype-specific cancer liabilities. *Cell* **163**, 1515–1526 (2015).
58. Jain, I. H. et al. Genetic screen for cell fitness in high or low oxygen highlights mitochondrial and lipid metabolism. *Cell* **181**, 716–727.e11 (2020).
59. Wang, T., Wei, J. J., Sabatini, D. M. & Lander, E. S. Genetic screens in human cells using the CRISPR–Cas9 system. *Science* **343**, 80–84 (2014).
60. Chavez, A. et al. Highly efficient Cas9-mediated transcriptional programming. *Nat. Methods* **12**, 326–328 (2015).
61. Konermann, S. et al. Genome-scale transcriptional activation by an engineered CRISPR–Cas9 complex. *Nature* **517**, 583–588 (2015).
62. Gao, Y. et al. Complex transcriptional modulation with orthogonal and inducible dCas9 regulators. *Nat. Methods* **13**, 1043–1049 (2016).
63. Gilbert, L. A. et al. CRISPR-mediated modular RNA-guided regulation of transcription in eukaryotes. *Cell* **154**, 442–451 (2013).
64. Polstein, L. R. & Gersbach, C. A. A light-inducible CRISPR–Cas9 system for control of endogenous gene activation. *Nat. Chem. Biol.* **11**, 198–200 (2015).
65. Qi, L. S. et al. Repurposing CRISPR as an RNA-guided platform for sequence-specific control of gene expression. *Cell* **152**, 1173–1183 (2013).
66. Tanenbaum, M. E., Gilbert, L. A., Qi, L. S., Weissman, J. S. & Vale, R. D. A protein-tagging system for signal amplification in gene expression and fluorescence imaging. *Cell* **159**, 635–646 (2014).
67. Zalatan, J. G. et al. Engineering complex synthetic transcriptional programs with CRISPR RNA scaffolds. *Cell* **160**, 339–350 (2015).
68. Alerasool, N., Segal, D., Lee, H. & Taipale, M. An efficient KRAB domain for CRISPRi applications in human cells. *Nat. Methods* **17**, 1093–1096 (2020).
69. Wang, H., La Russa, M. & Qi, L. S. CRISPR/Cas9 in genome editing and beyond. *Annu. Rev. Biochem.* **85**, 227–264 (2016).
70. Xu, X. & Qi, L. S. A CRISPR–dCas toolbox for genetic engineering and synthetic biology. *J. Mol. Biol.* **431**, 34–47 (2019).
71. Yeo, N. C. et al. An enhanced CRISPR repressor for targeted mammalian gene regulation. *Nat. Methods* **15**, 611–616 (2018).
72. Morgens, D. W. et al. Genome-scale measurement of off-target activity using Cas9 toxicity in high-throughput screens. *Nat. Commun.* **8**, 15178 (2017).
73. Rossi, A. et al. Genetic compensation induced by deleterious mutations but not gene knockdowns. *Nature* **524**, 230–233 (2015).
74. Nuñez, J. K. et al. Genome-wide programmable transcriptional memory by CRISPR-based epigenome editing. *Cell* **184**, 2503–2519.e17 (2021). **This study introduces the CRISPRoff method for epigenome editing, which enables stable, mitotically heritable silencing of target genes.**
75. Matharu, N. et al. CRISPR-mediated activation of a promoter or enhancer rescues obesity caused by haploinsufficiency. *Science* **363**, eaau0629 (2019).
76. Zetsche, B. et al. Cpf1 is a single RNA-guided endonuclease of a class 2 CRISPR–Cas system. *Cell* **163**, 759–771 (2015).
77. Liu, Y. et al. Engineering cell signaling using tunable CRISPR–Cpf1-based transcription factors. *Nat. Commun.* **8**, 2095 (2017).
78. Xu, X. et al. Engineered miniature CRISPR-Cas system for mammalian genome regulation and editing. *Mol. Cell* **81**, 4333–4345.e4 (2021).
79. Konermann, S. et al. Transcriptome engineering with RNA-targeting type VI-D CRISPR effectors. *Cell* **173**, 665–676.e14 (2018).
80. Wessels, H.-H. et al. Massively parallel Cas13 screens reveal principles for guide RNA design. *Nat. Biotechnol.* **38**, 722–727 (2020).
81. Du, M., Jillette, N., Zhu, J. J., Li, S. & Cheng, A. W. CRISPR artificial splicing factors. *Nat. Commun.* **11**, 2973 (2020).
82. Gapinske, M. et al. CRISPR-SKIP: programmable gene splicing with single base editors. *Genome Biol.* **19**, 107 (2018).
83. Mou, H. et al. CRISPR/Cas9-mediated genome editing induces exon skipping by alternative splicing or exon deletion. *Genome Biol.* **18**, 108 (2017).
84. Amabile, A. et al. Inheritable silencing of endogenous genes by hit-and-run targeted epigenetic editing. *Cell* **167**, 219–232.e14 (2016).
85. Braun, S. M. G. et al. Rapid and reversible epigenome editing by endogenous chromatin regulators. *Nat. Commun.* **8**, 560 (2017).
86. Hilton, I. B. et al. Epigenome editing by a CRISPR–Cas9-based acetyltransferase activates genes from promoters and enhancers. *Nat. Biotechnol.* **33**, 510–517 (2015).
87. Kearns, N. A. et al. Functional annotation of native enhancers with a Cas9–histone demethylase fusion. *Nat. Methods* **12**, 401–403 (2015).
88. Kim, J.-M. et al. Cooperation between SMDY3 and PC4 drives a distinct transcriptional program in cancer cells. *Nucleic Acids Res.* **43**, 8868–8883 (2015).
89. Kwon, D. Y., Zhao, Y.-T., Lamonica, J. M. & Zhou, Z. Locus-specific histone deacetylation using a synthetic CRISPR–Cas9-based HDAC. *Nat. Commun.* **8**, 15315 (2017).
90. O’Geen, H. et al. dCas9-based epigenome editing suggests acquisition of histone methylation is not sufficient for target gene repression. *Nucleic Acids Res.* **45**, 9901–9916 (2017).
91. Okada, M., Kanamori, M., Someya, K., Nakatsukasa, H. & Yoshimura, A. Stabilization of Foxp3 expression by CRISPR–dCas9-based epigenome editing in mouse primary T cells. *Epigenetics Chromatin* **10**, 24 (2017).
92. Stepper, P. et al. Efficient targeted DNA methylation with chimeric dCas9 — Dnmt3a — Dnmt3L methyltransferase. *Nucleic Acids Res.* **45**, 1703–1713 (2017).
93. Xu, X. et al. High-fidelity CRISPR/Cas9-based gene-specific hydroxymethylation rescues gene expression and attenuates renal fibrosis. *Nat. Commun.* **9**, 3509 (2018).
94. Kim, J. H. et al. LADL: light-activated dynamic looping for endogenous gene expression control. *Nat. Methods* **16**, 633–639 (2019).
95. Morgan, S. L. et al. Manipulation of nuclear architecture through CRISPR-mediated chromosomal looping. *Nat. Commun.* **8**, 15993 (2017).
96. Wang, H. et al. CRISPR-mediated programmable 3D genome positioning and nuclear organization. *Cell* **175**, 1405–1417.e14 (2018).
97. Liu, X. M., Zhou, J., Mao, Y., Ji, Q. & Qian, S. B. Programmable RNA<sup>m6</sup>-methyladenosine editing by CRISPR–Cas9 conjugates. *Nat. Chem. Biol.* **15**, 865–871 (2019).
98. O’Connell, M. R. et al. Programmable RNA recognition and cleavage by CRISPR/Cas9. *Nature* **516**, 263–266 (2014).
99. Rees, H. A. & Liu, D. R. Base editing: precision chemistry on the genome and transcriptome of living cells. *Nat. Rev. Genet.* **19**, 770–788 (2018).
100. Cheng, L. et al. Single-nucleotide-level mapping of DNA regulatory elements that control fetal hemoglobin expression. *Nat. Genet.* **53**, 869–880 (2021).
101. Gaudelli, N. M. et al. Programmable base editing of T to G in genomic DNA without DNA cleavage. *Nature* **551**, 464–471 (2017).
102. Komor, A. C. et al. Improved base excision repair inhibition and bacteriophage Mu Gam protein yields C:G-to-T:A base editors with higher efficiency and product purity. *Sci. Adv.* **3**, eaau4774 (2017).
103. Molla, K. A. & Yang, Y. CRISPR/Cas-mediated base editing: technical considerations and practical applications. *Trends Biotechnol.* **37**, 1121–1142 (2019).
104. Yeh, W.-H., Chiang, H., Rees, H. A., Edge, A. S. B. & Liu, D. R. In vivo base editing of post-mitotic sensory cells. *Nat. Commun.* **9**, 2184 (2018).
105. Koblan, L. W. et al. Efficient C•G-to-G•C base editors developed using CRISPRi screens, target-library analysis, and machine learning. *Nat. Biotechnol.* **39**, 1414–1425 (2021).
106. Arbab, M. et al. Determinants of base editing outcomes from target library analysis and machine learning. *Cell* **182**, 463–480.e30 (2020).
107. Gehrke, J. M. et al. An APOBEC3a–Cas9 base editor with minimized bystander and off-target activities. *Nat. Biotechnol.* **36**, 977 (2018).
108. Grünwald, J. et al. Transcriptome-wide off-target RNA editing induced by CRISPR-guided DNA base editors. *Nature* **569**, 433–437 (2019).
109. Cox, D. B. T. et al. RNA editing with CRISPR–Cas13. *Science* **358**, 1019–1027 (2017).
110. Abudayyeh, O. O. et al. A cytosine deaminase for programmable single-base RNA editing. *Science* **365**, 382–386 (2019).
111. Shi, J. et al. Discovery of cancer drug targets by CRISPR–Cas9 screening of protein domains. *Nat. Biotechnol.* **33**, 661–667 (2015).
112. Li, K., Wang, G., Andersen, T., Zhou, P. & Pu, W. T. Optimization of genome engineering approaches with the CRISPR/Cas9 system. *PLoS ONE* **9**, e105779 (2014).
113. Anzalone, A. V. et al. Search-and-replace genome editing without double-strand breaks or donor DNA. *Nature* **576**, 149–157 (2019). **This study describes CRISPR prime editing, which enables targeted introduction of short DNA sequences based on a single template.**
114. Chen, P. J. et al. Enhanced prime editing systems by manipulating cellular determinants of editing outcomes. *Cell* **184**, 5635–5652 (2021).
115. Nelson, J. W. et al. Engineered pegRNAs improve prime editing efficiency. *Nat. Biotechnol.* <https://doi.org/10.1038/s41587-021-01039-7> (2021).
116. Chow, R. D., Chen, J. S., Shen, J. & Chen, S. A web tool for the design of prime-editing guide RNAs. *Nat. Biomed. Eng.* **5**, 190–194 (2021).
117. Hsu, J. Y. et al. PrimeDesign software for rapid and simplified design of prime editing guide RNAs. *Nat. Commun.* **12**, 1034 (2021).
118. Kim, H. K. et al. Predicting the efficiency of prime editing guide RNAs in human cells. *Nat. Biotechnol.* **39**, 198–206 (2021).
119. Erwood, S. et al. Saturation variant interpretation using CRISPR prime editing. Preprint at *bioRxiv* <https://doi.org/10.1101/2021.05.11.443710v1> (2021).
120. Choi, J. et al. Precise genomic deletions using paired prime editing. *Nat. Biotechnol.* <https://doi.org/10.1038/s41587-021-01025-z> (2021).
121. Jiang, T., Zhang, X.-O., Weng, Z. & Xue, W. Deletion and replacement of long genomic sequences using prime editing. *Nat. Biotechnol.* <https://doi.org/10.1038/s41587-021-01026-y> (2021).
122. Anzalone, A. V. et al. Programmable deletion, replacement, integration and inversion of large DNA sequences with twin prime editing. *Nat. Biotechnol.* <https://doi.org/10.1038/s41587-021-01133-w> (2021).
123. Ioannidi, E. I. et al. Drag-and-drop genome insertion without DNA cleavage with CRISPR-directed integrases. Preprint at *bioRxiv* <https://doi.org/10.1101/2021.11.01.466786v1> (2021).
124. Potting, C. et al. Genome-wide CRISPR screen for PARKIN regulators reveals transcriptional repression as a determinant of mitophagy. *Proc. Natl Acad. Sci. USA* **115**, E180–E189 (2018).

125. Wong, N. M. et al. Engineering digitizer circuits for chemical and genetic screens in human cells. *Nat. Commun.* **12**, 6150 (2021).
126. Haney, M. S. et al. Identification of phagocytosis regulators using magnetic genome-wide CRISPR screens. *Nat. Genet.* **50**, 1716–1727 (2018).
127. Mair, B. et al. High-throughput genome-wide phenotypic screening via immunomagnetic cell sorting. *Nat. Biomed. Eng.* **3**, 796–805 (2019).
128. Mair, B. et al. Essential gene profiles for human pluripotent stem cells identify uncharacterized genes and substrate dependencies. *Cell Rep.* **27**, 599–615.e12 (2019).
129. Shifrut, E. et al. Genome-wide CRISPR screens in primary human T cells reveal key regulators of immune function. *Cell* **175**, 1958–1971.e15 (2018).
130. Dong, M. B. et al. Systematic immunotherapy target discovery using genome-scale in vivo CRISPR screens in CD8 T cells. *Cell* **178**, 1189–1204.e23 (2019). **This study highlights the feasibility of in vivo CRISPR screening in T cells and its utility for immunotherapy target discovery.**
131. Gurusamy, D. et al. Multi-phenotype CRISPR–Cas9 screen identifies p38 kinase as a target for adoptive immunotherapies. *Cancer Cell* **37**, 818–833.e9 (2020).
132. Shang, W. et al. Genome-wide CRISPR screen identifies FAM49B as a key regulator of actin dynamics and T cell activation. *Proc. Natl Acad. Sci. USA* **115**, E4051–E4060 (2018).
133. Chen, Z. et al. In vivo CD8<sup>+</sup> T cell CRISPR screening reveals control by Fli1 in infection and cancer. *Cell* **184**, 1262–1280.e22 (2021).
134. Henriksson, J. et al. Genome-wide CRISPR screens in T helper cells reveal pervasive crosstalk between activation and differentiation. *Cell* **176**, 882–896.e18 (2019).
135. LaFleur, M. W. et al. PTPN22 regulates the generation of exhausted CD8<sup>+</sup> T cell subpopulations and restrains tumor immunity. *Nat. Immunol.* **20**, 1355–1347 (2019).
136. Fulco, C. P. et al. Activity-by-contact model of enhancer-promoter regulation from thousands of CRISPR perturbations. *Nat. Genet.* **51**, 1664–1669 (2019).
137. Reilly, S. K. et al. Direct characterization of cis-regulatory elements and functional dissection of complex genetic associations using HCR–FlowFISH. *Nat. Genet.* **53**, 1166–1176 (2021).
138. Wroblewska, A. et al. Protein barcodes enable high-dimensional single-cell CRISPR screens. *Cell* **175**, 1141–1155.e16 (2018).
139. Adamson, B. et al. A multiplexed single-cell CRISPR screening platform enables systematic dissection of the unfolded protein response. *Cell* **167**, 1867–1882.e21 (2016).
140. Dixit, A. et al. Perturb-seq: dissecting molecular circuits with scalable single-cell RNA profiling of pooled genetic screens. *Cell* **167**, 1853–1866.e17 (2016).
141. Jaitin, D. A. et al. Dissecting immune circuits by linking CRISPR-pooled screens with single-cell RNA-seq. *Cell* **167**, 1883–1896.e15 (2016).
142. Datlinger, P. et al. Pooled CRISPR screening with single-cell transcriptome readout. *Nat. Methods* **14**, 297–301 (2017). **Together with Adamson et al. (2016), Dixit et al. (2016) and Jaitin et al. (2016), these studies introduce CRISPR screens with single-cell sequencing read-out as a broadly useful method for dissecting gene regulation and cell states.**
143. Xie, S., Duan, J., Li, B., Zhou, P. & Hon, G. C. Multiplexed engineering and analysis of combinatorial enhancer activity in single cells. *Mol. Cell* **66**, 285–299.e5 (2017).
144. Jin, X. et al. In vivo Perturb-seq reveals neuronal and glial abnormalities associated with autism risk genes. *Science* **370**, aaz6063 (2020).
145. Hill, A. J. et al. On the design of CRISPR-based single-cell molecular screens. *Nat. Methods* **15**, 271–274 (2018).
146. Adamson, B., Norman, T. M., Jost, M. & Weissman, J. S. Approaches to maximize sgRNA-barcode coupling in Perturb-seq screens. Preprint at *bioRxiv* <https://doi.org/10.1101/298349v1> (2018).
147. Mimitou, E. P. et al. Multiplexed detection of proteins, transcriptomes, clonotypes and CRISPR perturbations in single cells. *Nat. Methods* **16**, 409–412 (2019).
148. Replogle, J. M. et al. Combinatorial single-cell CRISPR screens by direct guide RNA capture and targeted sequencing. *Nat. Biotechnol.* **38**, 954–961 (2020).
149. Schraivogel, D. et al. Targeted Perturb-seq enables genome-scale genetic screens in single cells. *Nat. Methods* **17**, 629–635 (2020).
150. Cao, J. et al. The single-cell transcriptional landscape of mammalian organogenesis. *Nature* **566**, 496–502 (2019).
151. Rosenberg, A. B. et al. Single-cell profiling of the developing mouse brain and spinal cord with split-pool barcoding. *Science* **360**, 176–182 (2018).
152. Datlinger, P. et al. Ultra-high-throughput single-cell RNA sequencing and perturbation screening with combinatorial fluidic indexing. *Nat. Methods* **18**, 635–642 (2021).
153. Bock, C., Farlik, M. & Sheffield, N. C. Multi-omics of single cells: strategies and applications. *Trends Biotechnol.* **34**, 605–608 (2016).
154. Chappell, L., Russell, A. J. C. & Voet, T. Single-cell (multi)omics technologies. *Annu. Rev. Genomics Hum. Genet.* **19**, 15–41 (2018).
155. Lisovitch-Brauer, N. et al. Profiling the genetic determinants of chromatin accessibility with scalable single-cell CRISPR screens. *Nat. Biotechnol.* **39**, 1270–1277 (2021).
156. Pierce, S. E., Granja, J. M. & Greenleaf, W. J. High-throughput single-cell chromatin accessibility CRISPR screens enable unbiased identification of regulatory networks in cancer. *Nat. Commun.* **12**, 2969 (2021).
157. Rubin, A. J. et al. Coupled single-cell CRISPR screening and epigenomic profiling reveals causal gene regulatory networks. *Cell* **176**, 361–376.e17 (2019).
158. Frangieh, C. J. et al. Multimodal pooled Perturb-CITE-seq screens in patient models define mechanisms of cancer immune evasion. *Nat. Genet.* **53**, 332–341 (2021).
159. Papalexli, E. et al. Characterizing the molecular regulation of inhibitory immune checkpoints with multimodal single-cell screens. *Nat. Genet.* **53**, 322–331 (2021).
160. Lin, S., Schorpp, K., Rothenaigner, I. & Hadani, K. Image-based high-content screening in drug discovery. *Drug Discov. Today* **25**, 1348–1361 (2020).
161. Wheeler, E. C. et al. Pooled CRISPR screens with imaging on microarray reveals stress granule-regulatory factors. *Nat. Methods* **17**, 636–642 (2020).
162. Hasle, N. et al. High-throughput, microscope-based sorting to dissect cellular heterogeneity. *Mol. Syst. Biol.* **16**, e9442 (2020).
163. Kanfer, G. et al. Image-based pooled whole-genome CRISPRi screening for subcellular phenotypes. *J. Cell Biol.* **220**, e202006180 (2021).
164. Yan, X. et al. High-content imaging-based pooled CRISPR screens in mammalian cells. *J. Cell Biol.* **220**, e202008158 (2021).
165. Emanuel, G., Moffitt, J. R. & Zhuang, X. High-throughput, image-based screening of pooled genetic-variant libraries. *Nat. Methods* **14**, 1159–1162 (2017).
166. Lawson, M. J. et al. In situ genotyping of a pooled strain library after characterizing complex phenotypes. *Mol. Syst. Biol.* **13**, 947 (2017).
167. Camsund, D. et al. Time-resolved imaging-based CRISPRi screening. *Nat. Methods* **17**, 86–92 (2020).
168. Chen, K. H., Boettiger, A. N., Moffitt, J. R., Wang, S. & Zhuang, X. RNA imaging. Spatially resolved, highly multiplexed RNA profiling in single cells. *Science* **348**, aaa6090 (2015).
169. Wang, C., Lu, T., Emanuel, G., Babcock, H. P. & Zhuang, X. Imaging-based pooled CRISPR screening reveals regulators of lncRNA localization. *Proc. Natl Acad. Sci. USA* **116**, 10842–10851 (2019).
170. Feldman, D. et al. Optical pooled screens in human cells. *Cell* **179**, 787–799.e17 (2019). **Together with Camsund et al. (2020) and Wang et al. (2019), these studies demonstrate pooled CRISPR screening with spatial imaging read-outs.**
171. Ke, R. et al. In situ sequencing for RNA analysis in preserved tissue and cells. *Nat. Methods* **10**, 857–860 (2013).
172. Lee, J. H. et al. Highly multiplexed subcellular RNA sequencing in situ. *Science* **343**, 1360–1363 (2014).
173. Li, W. et al. MAGeCK enables robust identification of essential genes from genome-scale CRISPR/Cas9 knockout screens. *Genome Biol.* **15**, 554 (2014).
174. Meyers, R. M. et al. Computational correction of copy number effect improves specificity of CRISPR–Cas9 essentiality screens in cancer cells. *Nat. Genet.* **49**, 1779–1784 (2017).
175. Jeong, H.-H., Kim, S.-Y., Rousseaux, M. W. C., Zoghbi, H. Y. & Liu, Z.  $\beta$ -Binomial modeling of CRISPR pooled screen data identifies target genes with greater sensitivity and fewer false negatives. *Genome Res.* **29**, 999–1008 (2019).
176. Langmead, B. & Salzberg, S. L. Fast gapped-read alignment with Bowtie 2. *Nat. Methods* **9**, 357–359 (2012).
177. Li, H. & Durbin, R. Fast and accurate short read alignment with Burrows–Wheeler transform. *Bioinformatics* **25**, 1754–1760 (2009).
178. Luecken, M. D. & Theis, F. J. Current best practices in single-cell RNA-seq analysis: a tutorial. *Mol. Syst. Biol.* **15**, e8746 (2019).
179. Stuart, T. & Satija, R. Integrative single-cell analysis. *Nat. Rev. Genet.* **20**, 257–272 (2019).
180. Stuart, T. et al. Comprehensive integration of single-cell data. *Cell* **177**, 1888–1902.e21 (2019).
181. Wolf, F. A., Angerer, P. & Theis, F. J. ScanPy: large-scale single-cell gene expression data analysis. *Genome Biol.* **19**, 15 (2018).
182. Caicedo, J. C. et al. Data-analysis strategies for image-based cell profiling. *Nat. Methods* **14**, 849–863 (2017).
183. McQuin, C. et al. CellProfiler 3.0: next-generation image processing for biology. *PLoS Biol.* **16**, e2005970 (2018).
184. Pau, G., Fuchs, F., Sklyar, O., Boutros, M. & Huber, W. EImage — an R package for image processing with applications to cellular phenotypes. *Bioinformatics* **26**, 979–981 (2010).
185. Li, W. et al. Quality control, modeling, and visualization of CRISPR screens with MAGeCK-VISPR. *Genome Biol.* **16**, 281 (2015).
186. Hart, T., Brown, K. R., Sircoulomb, F., Rottapel, R. & Moffat, J. Measuring error rates in genomic perturbation screens: gold standards for human functional genomics. *Mol. Syst. Biol.* **10**, 733 (2014).
187. Daley, T. P. et al. CRISPhieRmix: a hierarchical mixture model for CRISPR pooled screens. *Genome Biol.* **19**, 159 (2018).
188. Hart, T. & Moffat, J. BAGEL: a computational framework for identifying essential genes from pooled library screens. *BMC Bioinformatics* **17**, 164 (2016).
189. Imkeller, K., Ambrosi, G., Boutros, M. & Huber, W. gscreen: modelling asymmetric count ratios in CRISPR screens to decrease experiment size and improve phenotype detection. *Genome Biol.* **21**, 53 (2020).
190. Gonçalves, E. et al. Structural rearrangements generate cell-specific, gene-independent CRISPR–Cas9 loss of fitness effects. *Genome Biol.* **20**, 27 (2019).
191. Iorio, F. et al. Unsupervised correction of gene-independent cell responses to CRISPR–Cas9 targeting. *BMC Genomics* **19**, 604 (2018).
192. Bodapati, S., Daley, T. P., Lin, X., Zou, J. & Qi, L. S. A benchmark of algorithms for the analysis of pooled CRISPR screens. *Genome Biol.* **21**, 62 (2020).
193. Allen, F. et al. JACKS: joint analysis of CRISPR/Cas9 knockout screens. *Genome Res.* **29**, 464–471 (2019).
194. Wang, B. et al. Integrative analysis of pooled CRISPR genetic screens using MAGeCKFlute. *Nat. Protoc.* **14**, 756–780 (2019).
195. Colic, M. et al. Identifying chemogenetic interactions from CRISPR screens with DrugZ. *Genome Med.* **11**, 52 (2019).
196. Burkhardt, D. B. et al. Quantifying the effect of experimental perturbations at single-cell resolution. *Nat. Biotechnol.* **39**, 619–629 (2021).
197. Duan, J. & Hon, G. FBA: feature barcoding analysis for single cell RNA-seq. *Bioinformatics* **22**, 4266–4268 (2021).
198. Liberzon, A. et al. The Molecular Signatures Database (MSigDB) hallmark gene set collection. *Cell Syst.* **1**, 417–425 (2015).
199. Szklarczyk, D. et al. The STRING database in 2017: quality-controlled protein–protein association networks, made broadly accessible. *Nucleic Acids Res.* **45**, D362–D368 (2017).
200. Kuleshov, M. V. et al. Enrichr: a comprehensive gene set enrichment analysis web server 2016 update. *Nucleic Acids Res.* **44**, W90–W97 (2016).
201. Sheffield, N. C. & Bock, C. LOLA: enrichment analysis for genomic region sets and regulatory elements in R and Bioconductor. *Bioinformatics* **32**, 587–589 (2016).
202. Grevet, J. D. et al. Domain-focused CRISPR screen identifies HRI as a fetal hemoglobin regulator in human erythroid cells. *Science* **361**, 285–290 (2018).

203. Sher, F. et al. Rational targeting of a NuRD subcomplex guided by comprehensive in situ mutagenesis. *Nat. Genet.* **51**, 1149–1159 (2019).
204. Dixon, G. et al. QSER1 protects DNA methylation valleys from de novo methylation. *Science* **372**, eabd0875 (2021).
205. Cheng, W. et al. CRISPR–Cas9 screens identify the RNA helicase DDX3X as a repressor of C9ORF72 (GGGGCC)<sub>n</sub> repeat-associated non-AUG translation. *Neuron* **104**, 885–898.e8 (2019).
206. Ebringt, R. Y. et al. Deregulation of ribosomal protein expression and translation promotes breast cancer metastasis. *Science* **367**, 1468–1473 (2020).
207. Breslow, D. K. et al. A CRISPR-based screen for Hedgehog signaling provides insights into ciliary function and ciliopathies. *Nat. Genet.* **50**, 460–471 (2018).
208. Pusapati, G. V. et al. CRISPR screens uncover genes that regulate target cell sensitivity to the morphogen Sonic Hedgehog. *Dev. Cell* **44**, 113–129.e8 (2018).
209. Chen, S. et al. Genome-wide CRISPR screen in a mouse model of tumor growth and metastasis. *Cell* **160**, 1246–1260 (2015).
210. Shalem, O. et al. Genome-scale CRISPR–Cas9 knockout screening in human cells. *Science* **343**, 84–87 (2014).
211. Li, Q. V. et al. Genome-scale screens identify JNK–JUN signaling as a barrier for pluripotency exit and endoderm differentiation. *Nat. Genet.* **51**, 999–1010 (2019).
212. Liu, Y. et al. CRISPR activation screens systematically identify factors that drive neuronal fate and reprogramming. *Cell Stem Cell* **23**, 758–771.e8 (2018).
213. Condon, K. J. et al. Genome-wide CRISPR screens reveal multitiered mechanisms through which mTORC1 senses mitochondrial dysfunction. *Proc. Natl Acad. Sci. USA* **118**, e2022120118 (2021).
214. Tian, R. et al. Genome-wide CRISPR/a screens in human neurons link lysosomal failure to ferroptosis. *Nat. Neurosci.* **24**, 1020–1034 (2021).
215. Morita, K. et al. Genome-wide CRISPR screen identifies TMEM41B as a gene required for autophagosome formation. *J. Cell Biol.* **217**, 3817–3828 (2018).
216. Shoemaker, C. J. et al. CRISPR screening using an expanded toolkit of autophagy reporters identifies TMEM41B as a novel autophagy factor. *PLoS Biol.* **17**, e2007044 (2019).
217. McFaline-Figueroa, J. L. et al. A pooled single-cell genetic screen identifies regulatory checkpoints in the continuum of the epithelial-to-mesenchymal transition. *Nat. Genet.* **51**, 1389–1398 (2019).
218. Dede, M., McLaughlin, M., Kim, E. & Hart, T. Multiplex enCas12a screens detect functional buffering among paralogs otherwise masked in monogenic Cas9 knockout screens. *Genome Biol.* **21**, 262 (2020).
219. De Kegel, B. & Ryan, C. J. Paralog buffering contributes to the variable essentiality of genes in cancer cell lines. *PLoS Genet.* **15**, e1008466 (2019).
220. Wang, T. et al. Gene essentiality profiling reveals gene networks and synthetic lethal interactions with oncogenic ras. *Cell* **168**, 890–903.e15 (2017).
221. Wang, T. et al. Identification and characterization of essential genes in the human genome. *Science* **350**, 1096–1101 (2015).
222. Badano, J. L. & Katsanis, N. Beyond Mendel: an evolving view of human genetic disease transmission. *Nat. Rev. Genet.* **3**, 779–789 (2002).
223. Gurdasani, D., Barroso, I., Zeggini, E. & Sandhu, M. S. Genomics of disease risk in globally diverse populations. *Nat. Rev. Genet.* **20**, 520–535 (2019).
224. Huang, A., Garraway, L. A., Ashworth, A. & Weber, B. Synthetic lethality as an engine for cancer drug target discovery. *Nat. Rev. Drug Discov.* **19**, 23–38 (2020).
225. Norman, T. M. et al. Exploring genetic interaction manifolds constructed from rich single-cell phenotypes. *Science* **365**, 786–795 (2019).
226. Gupta, A. et al. Deep learning in image cytometry: a review. *Cytometry A* **95**, 366–380 (2019).
227. Lotfollahi, M., Wolf, F. A. & Theis, F. J. scGen predicts single-cell perturbation responses. *Nat. Methods* **16**, 715–721 (2019).
228. Shendure, J. & Fields, S. Massively parallel genetics. *Genetics* **203**, 617–619 (2016).
229. Findlay, G. M. et al. Accurate classification of BRCA1 variants with saturation genome editing. *Nature* **562**, 217–222 (2018).
230. Hanna, R. E. et al. Massively parallel assessment of human variants with base editor screens. *Cell* **184**, 1064–1080.e20 (2021).
- This study demonstrates that CRISPR screens with base editing are feasible and useful for characterizing genetic variants.**
231. Kweon, J. et al. A CRISPR-based base-editing screen for the functional assessment of BRCA1 variants. *Oncogene* **39**, 30–35 (2020).
232. Cuella-Martin, R. et al. Functional interrogation of DNA damage response variants with base editing screens. *Cell* **184**, 1081–1097.e19 (2021).
233. Canver, M. C. et al. BCL11A enhancer dissection by Cas9-mediated in situ saturating mutagenesis. *Nature* **527**, 192–197 (2015).
234. Tsherniak, A. et al. Defining a cancer dependency map. *Cell* **170**, 564–576.e16 (2017).
235. Dempster, J. M. et al. Agreement between two large pan-cancer CRISPR–Cas9 gene dependency data sets. *Nat. Commun.* **10**, 5817 (2019).
- This study shows that CRISPR screens in cancer cell lines can yield consistent and reproducible results across different centres.**
236. Aregger, M. et al. Systematic mapping of genetic interactions for de novo fatty acid synthesis identifies C12orf49 as a regulator of lipid metabolism. *Nat. Metab.* **2**, 499–513 (2020).
237. Zamanighomi, M. et al. GEMINI: a variational Bayesian approach to identify genetic interactions from combinatorial CRISPR screens. *Genome Biol.* **20**, 137 (2019).
238. Bryant, H. E. et al. Specific killing of BRCA2-deficient tumours with inhibitors of poly(ADP-ribose) polymerase. *Nature* **434**, 913–917 (2005).
239. Farmer, H. et al. Targeting the DNA repair defect in BRCA mutant cells as a therapeutic strategy. *Nature* **434**, 917–921 (2005).
240. Chan, E. M. et al. WRN helicase is a synthetic lethal target in microsatellite unstable cancers. *Nature* **568**, 551–556 (2019).
241. Kategaya, L., Perumal, S. K., Hager, J. H. & Belmont, L. D. Werner syndrome helicase is required for the survival of cancer cells with microsatellite instability. *iScience* **13**, 488–497 (2019).
242. Lieb, S. et al. Werner syndrome helicase is a selective vulnerability of microsatellite instability-high tumor cells. *eLife* **8**, e43333 (2019).
243. Lopes, R. et al. Systematic dissection of transcriptional regulatory networks by genome-scale and single-cell CRISPR screens. *Sci. Adv.* **7**, eabf5733 (2021).
244. Panganiban, R. A. et al. Genome-wide CRISPR screen identifies suppressors of endoplasmic reticulum stress-induced apoptosis. *Proc. Natl Acad. Sci. USA* **116**, 13584–13593 (2019).
245. Kamber, R. A. et al. Inter-cellular CRISPR screens reveal regulators of cancer cell phagocytosis. *Nature* **597**, 549–554 (2021).
246. Sheffer, M. et al. Genome-scale screens identify factors regulating tumor cell responses to natural killer cells. *Nat. Genet.* **53**, 1196–1206 (2021).
247. Hussmann, J. A. et al. Mapping the genetic landscape of DNA double-strand break repair. *Cell* **184**, 5653–5669 (2021).
248. Olivieri, M. et al. A genetic map of the response to DNA damage in human cells. *Cell* **182**, 481–496.e21 (2020).
249. Manguso, R. T. et al. In vivo CRISPR screening identifies Ptpn2 as a cancer immunotherapy target. *Nature* **547**, 413–418 (2017).
250. Artegiani, B. et al. Fast and efficient generation of knock-in human organoids using homology-independent CRISPR–Cas9 precision genome editing. *Nat. Cell Biol.* **22**, 321–331 (2020).
251. Han, K. et al. CRISPR screens in cancer spheroids identify 3D growth-specific vulnerabilities. *Nature* **580**, 136–141 (2020).
252. Pan, D. et al. A major chromatin regulator determines resistance of tumor cells to T cell-mediated killing. *Science* **359**, 770–775 (2018).
253. Hess, C. T. et al. Directed evolution using dCas9-targeted somatic hypermutation in mammalian cells. *Nat. Methods* **13**, 1036–1042 (2016).
254. Sanjana, N. E., Shalem, O. & Zhang, F. Improved vectors and genome-wide libraries for CRISPR screening. *Nat. Methods* **11**, 783–784 (2014).
255. Schumann, K. et al. Functional CRISPR dissection of gene networks controlling human regulatory T cell identity. *Nat. Immunol.* **21**, 1456–1466 (2020).
256. Wei, J. et al. Targeting REGNASE-1 programs long-lived effector T cells for cancer therapy. *Nature* **576**, 471–476 (2019).
257. Ye, L. et al. In vivo CRISPR screening in CD8 T cells with AAV–Sleeping Beauty hybrid vectors identifies membrane targets for improving immunotherapy for glioblastoma. *Nat. Biotechnol.* **37**, 1302–1313 (2019).
258. Parnas, O. et al. A genome-wide CRISPR screen in primary immune cells to dissect regulatory networks. *Cell* **162**, 675–686 (2015).
259. Covarrubias, S. et al. High-throughput CRISPR screening identifies genes involved in macrophage viability and inflammatory pathways. *Cell Rep.* **33**, 108541 (2020).
260. Schmid-Burgk, J. L. et al. A genome-wide CRISPR (clustered regularly interspaced short palindromic repeats) screen identifies NEK7 as an essential component of NLRP3 inflammasome activation. *J. Biol. Chem.* **291**, 103–109 (2016).
261. Baggen, J. et al. Genome-wide CRISPR screening identifies TMEM106B as a proviral host factor for SARS-CoV-2. *Nat. Genet.* **53**, 435–444 (2021).
262. Daniloski, Z. et al. Identification of required host factors for SARS-CoV-2 infection in human cells. *Cell* **184**, 92–105.e16 (2021).
263. Flynn, R. A. et al. Discovery and functional interrogation of SARS-CoV-2 RNA–host protein interactions. *Cell* **184**, 2394–2411.e16 (2021).
264. Hoffmann, M., Kleine-Weber, H. & Pöhlmann, S. A multibasic cleavage site in the spike protein of SARS-CoV-2 is essential for infection of human lung cells. *Mol. Cell* **78**, 779–784.e5 (2020).
265. Hoffmann, H.-H. et al. TMEM41B is a pan-flavivirus host factor. *Cell* **184**, 133–148.e20 (2021).
266. Schneider, W. M. et al. Genome-scale identification of SARS-CoV-2 and pan-coronavirus host factor networks. *Cell* **184**, 120–132.e14 (2021).
267. Wang, R. et al. Genetic screens identify host factors for SARS-CoV-2 and common cold coronaviruses. *Cell* **184**, 106–119.e14 (2021).
268. Wei, J. et al. Genome-wide CRISPR screens reveal host factors critical for SARS-CoV-2 infection. *Cell* **184**, 76–91.e13 (2021).
269. Zhu, Y. et al. A genome-wide CRISPR screen identifies host factors that regulate SARS-CoV-2 entry. *Nat. Commun.* **12**, 961 (2021).
270. Theisen, D. J. et al. WDFY4 is required for cross-presentation in response to viral and tumor antigens. *Science* **362**, 694–699 (2018).
271. Wei, S. C., Duffy, C. R. & Allison, J. P. Fundamental mechanisms of immune checkpoint blockade therapy. *Cancer Discov.* **8**, 1069–1086 (2018).
272. Huang, H. et al. In vivo CRISPR screening reveals nutrient signaling processes underpinning CD8<sup>+</sup> T cell fate decisions. *Cell* **184**, 1245–1261.e21 (2021).
273. Wang, X. et al. In vivo CRISPR screens identify the E3 ligase Cop1 as a modulator of macrophage infiltration and cancer immunotherapy target. *Cell* **184**, 5357–5374.e22 (2021).
274. Guil-Luna, S., Sedlik, C. & Piaggio, E. Humanized mouse models to evaluate cancer immunotherapeutics. *Annu. Rev. Cancer Biol.* **5**, 119–136 (2021).
275. Masopust, D. & Soerens, A. G. Tissue-resident T cells and other resident leukocytes. *Annu. Rev. Immunol.* **37**, 521–546 (2019).
276. Krausgruber, T. et al. Structural cells are key regulators of organ-specific immune responses. *Nature* **583**, 296–302 (2020).
277. Heng, T. S. P. & Painter, M. W. & Immunological Genome Project Consortium. The Immunological Genome Project: networks of gene expression in immune cells. *Nat. Immunol.* **9**, 1091–1094 (2008).
278. Regev, A. et al. The Human Cell Atlas. *eLife* **6**, e27041 (2017).
279. Adams, D. et al. BLUEPRINT to decode the epigenetic signature written in blood. *Nat. Biotechnol.* **30**, 224–226 (2012).
280. Shapiro, R. S., Chavez, A. & Collins, J. J. CRISPR-based genomic tools for the manipulation of genetically intractable microorganisms. *Nat. Rev. Microbiol.* **16**, 333–339 (2018).
281. Todor, H., Silvis, M. R., Osadnik, H. & Gross, C. A. Bacterial CRISPR screens for gene function. *Curr. Opin. Microbiol.* **59**, 102–109 (2021).
282. Wang, T. et al. Pooled CRISPR interference screening enables genome-scale functional genomics study in bacteria with superior performance. *Nat. Commun.* **9**, 2475 (2018).
283. Rousset, F. et al. Genome-wide CRISPR–dCas9 screens in *E. coli* identify essential genes and phase host factors. *PLoS Genet.* **14**, e1007749 (2018).
284. Peters, J. M. et al. A comprehensive, CRISPR-based functional analysis of essential genes in bacteria. *Cell* **165**, 1495–1506 (2016).

285. Peters, J. M. et al. Enabling genetic analysis of diverse bacteria with mobile-CRISPRi. *Nat. Microbiol.* **4**, 244–250 (2019).
286. Rousset, F. et al. The impact of genetic diversity on gene essentiality within the *Escherichia coli* species. *Nat. Microbiol.* **6**, 301–312 (2021).
287. Wet, T. Jde et al. Arrayed CRISPRi and quantitative imaging describe the morphotypic landscape of essential mycobacterial genes. *eLife* **9**, e00083 (2020).
288. Lee, H. H. et al. Functional genomics of the rapidly replicating bacterium *Vibrio natriegens* by CRISPRi. *Nat. Microbiol.* **4**, 1105–1113 (2019).
289. Strich, J. R. & Chertow, D. S. CRISPR–Cas biology and its application to infectious diseases. *J. Clin. Microbiol.* **57**, e01307–e01318 (2019).
290. Liu, X. et al. Exploration of bacterial bottlenecks and *Streptococcus pneumoniae* pathogenesis by CRISPRi-seq. *Cell Host Microbe* **29**, 107–120.e6 (2021).
291. Morio, F., Lombardi, L. & Butler, G. The CRISPR toolbox in medical mycology: state of the art and perspectives. *PLoS Pathog.* **16**, e1008201 (2020).
292. Bryant, J. M., Baumgarten, S., Glover, L., Hutchinson, S. & Rachidi, N. CRISPR in parasitology: not exactly cut and dried! *Trends Parasitol.* **35**, 409–422 (2019).
293. Sidik, S. M. et al. A genome-wide CRISPR screen in *Toxoplasma* identifies essential apicomplexan genes. *Cell* **166**, 1423–1435.e12 (2016).
294. Young, J. et al. A CRISPR platform for targeted in vivo screens identifies *Toxoplasma gondii* virulence factors in mice. *Nat. Commun.* **10**, 3963 (2019).
295. Rosiana, S. et al. Comprehensive genetic analysis of adhesin proteins and their role in virulence of *Candida albicans*. *Genetics* **217**, iyab003 (2021).
296. Shapiro, R. S. et al. A CRISPR–Cas9-based gene drive platform for genetic interaction analysis in *Candida albicans*. *Nat. Microbiol.* **3**, 73–82 (2018).
297. Li, Z. & Kim, K. S. RELATE enables genome-scale engineering in fungal genomics. *Sci. Adv.* **6**, eabb8783 (2020).
298. Caro, F., Place, N. M. & Mekalanos, J. J. Analysis of lipoprotein transport depletion in *Vibrio cholerae* using CRISPRi. *Proc. Natl Acad. Sci. USA* **116**, 17013–17022 (2019).
299. Liu, X. et al. High-throughput CRISPRi phenotyping identifies new essential genes in *Streptococcus pneumoniae*. *Mol. Syst. Biol.* **13**, 931 (2017).
300. Shields, R. C. et al. Repurposing the *Streptococcus mutans* CRISPR–Cas9 system to understand essential gene function. *PLoS Pathog.* **16**, e1008344 (2020).
301. Jaffe, M. et al. Improved discovery of genetic interactions using CRISPRiSeq across multiple environments. *Genome Res.* **29**, 668–681 (2019).
302. Jiang, W., Oikonomou, P. & Tavazoie, S. Comprehensive genome-wide perturbations via CRISPR adaptation reveal complex genetics of antibiotic sensitivity. *Cell* **180**, 1002–1017.e31 (2020).
303. Halder, V., McDonnell, B., Uthayakumar, D., Usher, J. & Shapiro, R. S. Genetic interaction analysis in microbial pathogens: unravelling networks of pathogenesis, antimicrobial susceptibility and host interactions. *FEMS Microbiol. Rev.* **45**, fuaa055 (2020).
304. Garst, A. D. et al. Genome-wide mapping of mutations at single-nucleotide resolution for protein, metabolic and genome engineering. *Nat. Biotechnol.* **35**, 48–55 (2017).
305. Mutalik, V. K. et al. High-throughput mapping of the phage resistance landscape in *E. coli*. *PLoS Biol.* **18**, e3000877 (2020).
306. Hein, M. Y. & Weissman, J. S. Functional single-cell genomics of human cytomegalovirus infection. *Nat. Biotechnol.* <https://doi.org/10.1038/s41587-021-01059-3> (2021).
307. Bao, Z. et al. Genome-scale engineering of *Saccharomyces cerevisiae* with single-nucleotide precision. *Nat. Biotechnol.* **36**, 505–508 (2018).
308. Donati, S. et al. Multi-omics analysis of CRISPRi-knockdowns identifies mechanisms that buffer decreases of enzymes in *E. coli* metabolism. *Cell Syst.* **12**, 56–67.e6 (2021).
309. Li, S. et al. Genome-wide CRISPRi-based identification of targets for decoupling growth from production. *ACS Synth. Biol.* **9**, 1030–1040 (2020).
310. Yao, L. et al. Pooled CRISPRi screening of the cyanobacterium *Synechocystis* sp PCC 6803 for enhanced industrial phenotypes. *Nat. Commun.* **11**, 1666 (2020).
311. Bowman, E. K. et al. Bidirectional titration of yeast gene expression using a pooled CRISPR guide RNA approach. *Proc. Natl Acad. Sci. USA* **117**, 18424–18430 (2020).
312. Hawkins, J. S. et al. Mismatch-CRISPRi reveals the co-varying expression–fitness relationships of essential genes in *Escherichia coli* and *Bacillus subtilis*. *Cell Syst.* **11**, 523–535 (2020).
313. Beuter, D. et al. Selective enrichment of slow-growing bacteria in a metabolism-wide CRISPRi library with a TIMER protein. *ACS Synth. Biol.* **7**, 2775–2782 (2018).
314. Guo, X. et al. High-throughput creation and functional profiling of DNA sequence variant libraries using CRISPR–Cas9 in yeast. *Nat. Biotechnol.* **36**, 540–546 (2018).
315. Després, P. C., Dubé, A. K., Seki, M., Yachie, N. & Landry, C. R. Perturbing proteomes at single residue resolution using base editing. *Nat. Commun.* **11**, 1871 (2020).
316. Köster, J. & Rahmann, S. Snakemake — a scalable bioinformatics workflow engine. *Bioinformatics* **28**, 2520–2522 (2012).
317. Cui, Y. et al. CRISPR-view: a database of functional genetic screens spanning multiple phenotypes. *Nucleic Acids Res.* **49**, D848–D854 (2021).
318. Oughtred, R. et al. The BioGRID interaction database: 2019 update. *Nucleic Acids Res.* **47**, D529–D541 (2019).
319. Liu, H. et al. CRISPR-ERA: a comprehensive design tool for CRISPR-mediated gene editing, repression and activation. *Bioinformatics* **31**, 3676–3678 (2015).
320. Galonska, C. et al. Genome-wide tracking of dCas9–methyltransferase footprints. *Nat. Commun.* **9**, 597 (2018).
321. Michlits, G. et al. CRISPR-UMI: single-cell lineage tracing of pooled CRISPR–Cas9 screens. *Nat. Methods* **14**, 1191–1197 (2017).
322. Schmierer, B. et al. CRISPR/Cas9 screening using unique molecular identifiers. *Mol. Syst. Biol.* **13**, 945 (2017).
323. Esk, C. et al. A human tissue screen identifies a regulator of ER secretion as a brain-size determinant. *Science* **370**, 935–941 (2020).
324. Michels, B. E. et al. Pooled in vitro and in vivo CRISPR–Cas9 screening identifies tumor suppressors in human colon organoids. *Cell Stem Cell* **26**, 782–792.e7 (2020).
325. Ringel, T. et al. Genome-scale CRISPR screening in human intestinal organoids identifies drivers of TGF- $\beta$  resistance. *Cell Stem Cell* **26**, 431–440.e8 (2020).
326. Allen, T. M. et al. Humanized immune system mouse models: progress, challenges and opportunities. *Nat. Immunol.* **20**, 770–774 (2019).
327. Walsh, N. C. et al. Humanized mouse models of clinical disease. *Annu. Rev. Pathol.* **12**, 187–215 (2017).
328. Kim, E. & Hart, T. Improved analysis of CRISPR fitness screens and reduced off-target effects with the BAGEL2 gene essentiality classifier. *Genome Med.* **13**, 2 (2021).
329. Hsu, J. Y. et al. CRISPR-SURF: discovering regulatory elements by deconvolution of CRISPR tiling screen data. *Nat. Methods* **15**, 992–993 (2018).
330. Dempster, J. M. et al. Chronos: a cell population dynamics model of CRISPR experiments that improves inference of gene fitness effects. *Genome Biol.* **22**, 343 (2021).
331. Vinceti, A. et al. CoRe: a robustly benchmarked R package for identifying core-fitness genes in genome-wide pooled CRISPR–Cas9 screens. *BMC Genomics* **17**, 22 (2021).
332. Ward, H. N. et al. Analysis of combinatorial CRISPR screens with the Orthrus scoring pipeline. *Nat. Protoc.* **16**, 4766–4798 (2021).
333. Duan, B. et al. Model-based understanding of single-cell CRISPR screening. *Nat. Commun.* **10**, 2233 (2019).
334. Wang, L. Single-cell normalization and association testing unifying CRISPR screen and gene co-expression analyses with Normalizr. *Nat. Commun.* **12**, 6395 (2021).
335. Yang, L. et al. scMAGECK links genotypes with multiple phenotypes in single-cell CRISPR screens. *Genome Biol.* **21**, 19 (2020).
336. Beneke, T. et al. Genetic dissection of a *Leishmania flagellar* proteome demonstrates requirement for directional motility in sand fly infections. *PLoS Pathog.* **15**, e1007828 (2019).

#### Acknowledgements

The authors thank D. Seruggia for critical reading of the manuscript. C.B. is supported by a European Research Council (ERC) Starting Grant (no. 679146) and Consolidator Grant (no. 101001971) of the European Union's Horizon 2020 Research and Innovation Programme. G.S. and L.S.Q. are supported by the Li Ka Shing Foundation, the US NIH Common Fund 4D Nucleome Program (U01 EB021240) and a US National Science Foundation CAREER award (award no. 2046650; L.S.Q.). R.S.S. is supported by a Canadian Institutes of Health Research (CIHR) Project Grant (PJT 162195). J.S., J.S.W. and X.Z. are Howard Hughes Medical Institute investigators.

#### Author contributions

Introduction (C.B.); Experimentation (C.B., P.D., F.C., M.A.C., M.B.D., K.A.L., T.L., T.M.N., G.S., S.C., M.G., J.M., L.S.Q., J.S., J.S.W. and X.Z.); Results (C.B., B.S., G.S., W.L. and L.S.Q.); Applications (C.B., F.C., M.A.C., M.B.D., K.A.L., L.M., T.M.N., S.C., M.G., J.M., R.S.S., J.S. and J.S.W.); Reproducibility and data deposition (C.B., B.S., G.S., W.L. and L.S.Q.); Limitations and optimizations (C.B.); Outlook (C.B.); Figures (C.B., P.D., L.M., B.S., W.L. and R.S.S.); Overview of the Primer (C.B.); Editing (all authors).

#### Competing interests

C.B. is a co-founder and scientific advisor of Aelian Biotechnology and NeuroLentech. S.C. is a co-founder of EvolveImmune Therapeutics and CellInfinity Bio. M.G. has performed consultancy for Sanofi, receives research funding from AstraZeneca and GlaxoSmithKline, and is a co-founder of Mosaic Therapeutics. J.M. is a shareholder of Northern Biologics and Pionyr Immunotherapeutics, and a scientific advisor and shareholder of Century Therapeutics and Aelian Biotechnology. L.S.Q. is a co-founder and scientific advisor of Epicrispr Biotechnologies and Refuge Biotechnologies. J.S. is a scientific advisor of Maze Therapeutics, Camp4 Therapeutics, Cajal Biosciences, Adaptive Biotechnologies and Guardant Health, and a co-founder of Scale Bio and Phase Genomics. J.S.W. consults for and holds equity in KSQ Therapeutics, Maze Therapeutics and Tenaya Therapeutics, is a venture partner at SAM Ventures and is a member of the Amgen Scientific Advisory Board. X.Z. is a co-founder and consultant of Vizgen. The other authors declare no competing interests.

#### Peer review information

*Nature Reviews Methods Primers* thanks Sabrina D'Agosto, Francesco Iorio and the other, anonymous, reviewer(s) for their contribution to the peer review of this work.

#### Publisher's note

Springer Nature remains neutral with regard to jurisdictional claims in published maps and institutional affiliations.

#### RELATED LINKS

Addgene: <https://www.addgene.org/>  
 DepMap: <https://depmap.org/>  
 EBI ArrayExpress: <https://www.ebi.ac.uk/arrayexpress/>  
 EBI European Genome-phenome Archive (EGA): <https://ega-archive.org/>  
 International Nucleotide Sequence Database Collaboration: <https://www.insdc.org/>  
 NCBI database of Genotypes and Phenotypes (dbGAP): <https://www.ncbi.nlm.nih.gov/gap/>  
 NCBI Gene Expression Omnibus (GEO): <https://www.ncbi.nlm.nih.gov/geo/>  
 Zenodo: <https://zenodo.org/>

© Springer Nature Limited 2022